

Intracontinental deformation in southern Africa during the Late Cretaceous



Roderick Brown^{a,*}, Michael Summerfield^b, Andrew Gleadow^c, Kerry Gallagher^d, Andrew Carter^e, Romain Beucher^{a,1}, Mark Wildman^a

^a School of Geographical and Earth Sciences, College of Science and Engineering, University of Glasgow, Gregory Building, Glasgow G12 8QQ, Scotland, United Kingdom

^b School of Geosciences, Institute of Geography and Lived Environment, The University of Edinburgh, Drummond Street, Edinburgh EH8 9XP, Scotland, United Kingdom

^c School of Earth Sciences, University of Melbourne, Melbourne 3010, Australia

^d Géosciences Rennes, Université de Rennes 1, Campus de Beaulieu, 35042 Rennes, France

^e Department of Earth and Planetary Sciences, Birkbeck, University of London, Malet Street, WC1E 7HX, United Kingdom

ARTICLE INFO

Article history:

Received 13 September 2013

Received in revised form 17 May 2014

Accepted 19 May 2014

Available online 12 June 2014

Keywords:

Thermochronology

Intracontinental deformation

Apatite fission track analysis

Namibia

Africa

South Atlantic

ABSTRACT

Intracontinental deformation accommodated along major lithospheric scale shear zone systems and within associated extensional basins has been well documented within West, Central and East Africa during the Late Cretaceous. The nature of this deformation has been established by studies of the tectonic architecture of sedimentary basins preserved in this part of Africa. In southern Africa, where the post break-up history has been dominated by major erosion, little evidence for post-break-up tectonics has been preserved in the onshore geology. Here we present the results of 38 new apatite fission track analyses from the Damara region of northern Namibia and integrate these new data with our previous results that were focused on specific regions or sections only to comprehensively document the thermo-tectonic history of this region since continental break-up in the Early Cretaceous. The apatite fission track ages range from 449 ± 20 Ma to 59 ± 3 Ma, with mean confined track lengths between 14.61 ± 0.1 μm (SD 0.95 μm) to 10.83 ± 0.33 μm (SD 2.84 μm). The youngest ages (c. 80–60 Ma) yield the longest mean track lengths, and combined with their spatial distribution, indicate major cooling during the latest Cretaceous. A simple numerical thermal model is used to demonstrate that this cooling is consistent with the combined effects of heating caused by magmatic underplating, related to the Paraná-Etendeka continental flood volcanism associated with rifting and the opening of the South Atlantic, and enhanced erosion caused by major reactivation of major lithospheric structures within southern Africa during a key period of plate kinematic change that occurred in the South Atlantic and SW Indian ocean basins between 87 and 56 Ma. This phase of intraplate tectonism in northern Namibia, focused in discrete structurally defined zones, is coeval with similar phases elsewhere in Africa and suggests some form of trans-continental linkage between these lithospheric zones.

© 2014 The Authors. Published by Elsevier Ltd. This is an open access article under the CC BY license (<http://creativecommons.org/licenses/by/3.0/>).

1. Introduction

The influence of pre-existing lithospheric structure on the geometry and location of intra-continental rifting, associated with the development of the Atlantic Ocean, has been particularly well documented by studies in northeastern Brazil and in West, Central and East Africa (e.g. Burke and Dewey, 1974; Burke, 1976a, 1976b; McConnel, 1980; Pindell and Dewey, 1982; Fairhead and Okereke, 1987; Fairhead, 1988; Unternehr et al., 1988; Sénant and Popoff,

1991; Fairhead and Binks, 1991; Binks and Fairhead, 1992; McGargue et al., 1992; Maurin and Guiraud, 1993; Winn et al., 1993; Loule and Pospisil, 2012). These studies have highlighted the genetic relationship between the tectonic development of intracontinental rift basins, within Africa and South America, and changes in the nature and geometry of the surrounding plate boundaries, in particular those associated with the development of the North and Central Atlantic Ocean basins, from their initiation during the Late Triassic (e.g. Manspeizer, 1988; Torsvik et al., 2009) through to the present (Blundell, 1976).

Two Late Mesozoic tectonic episodes, characterised by major intracontinental deformation involving rifting and basin inversion, have been identified within West, Central and East Africa; one during the Early Cretaceous (~130 Ma) associated with continental

* Corresponding author. Tel.: +44 141 3305460.

E-mail address: roderick.brown@glasgow.ac.uk (R. Brown).

¹ Current address: Department of Earth Science, Faculty of Mathematics and Natural Sciences, University of Bergen, 5020 Bergen, Norway.

break-up and onset of sea floor spreading between Africa and South America and a second during the Late Cretaceous (~75–80 Ma), associated with a major change in the spreading geometry within the Central and South Atlantic Oceans (Klitgord and Schouten, 1986; Cande et al., 1988; Fairhead, 1988; Shaw and Cande, 1990; Dypvik et al., 1990; Binks and Fairhead, 1992; Bosworth, 1992; Fairhead and Binks, 1991; Guiraud and Maurin, 1992; Guiraud et al., 1992). Recognition of these Late Mesozoic episodes of tectonism, in West and Central Africa, was made possible largely by the sedimentary sequences, preserved within the intra-continental rift basins, providing a record of the basins' tectonic history. However, the paucity of Late Mesozoic and Tertiary age rocks preserved within southern Africa has prohibited any detailed study of the post-Gondwana (Late Mesozoic-Tertiary) tectonic development of this region.

Given this situation, apatite fission track analysis (AFTA) offers a unique opportunity for studying the Late Mesozoic and Tertiary tectonic and geomorphic history of southern Africa due to the technique's ability to document the low temperature (<~125 °C) thermal history of the crust (Brown et al., 1994a; Gallagher et al., 1998; Gleadow and Brown, 2000; Reiners et al., 2005; Reiners and Brandon, 2006). Significantly, AFTA results from the rift-margin of the Anza graben in Central Kenya (Foster and Gleadow, 1992, 1993, 1996) document at least two discrete pulses of denudational

cooling of the crust; one during the Early Cretaceous and a later episode during the Late Cretaceous–Palaeocene. The 38 new AFTA data reported here record a very similar chronology of shallow crustal cooling to that in Central Kenya, and when integrated with our earlier data (Raab et al., 2002, 2005) from this region provide strong support for the concept of a distinct tectonic episode affecting the interior of northern Namibia during the Late Cretaceous. The coincidence between this proposed period of tectonism in southwestern Africa and the Late Cretaceous episode identified in West, Central and East Africa (e.g. Fairhead, 1988; Fairhead and Binks, 1991; Binks and Fairhead, 1992), combined with the regional structural setting provides compelling evidence for a Late Cretaceous, trans-African ('neo-Pan-African') intracontinental tectonic episode. In this paper we report the new AFTA results and an integrated interpretation including previously published apatite fission track age data (Haack, 1976, 1983; Raab et al., 2002, 2005).

2. Regional tectonic setting and geology of northern Namibia

2.1. Tectonic setting

The regional crustal structure and topography of northern Namibia (Fig. 1) is dominated by the structural fabric of the

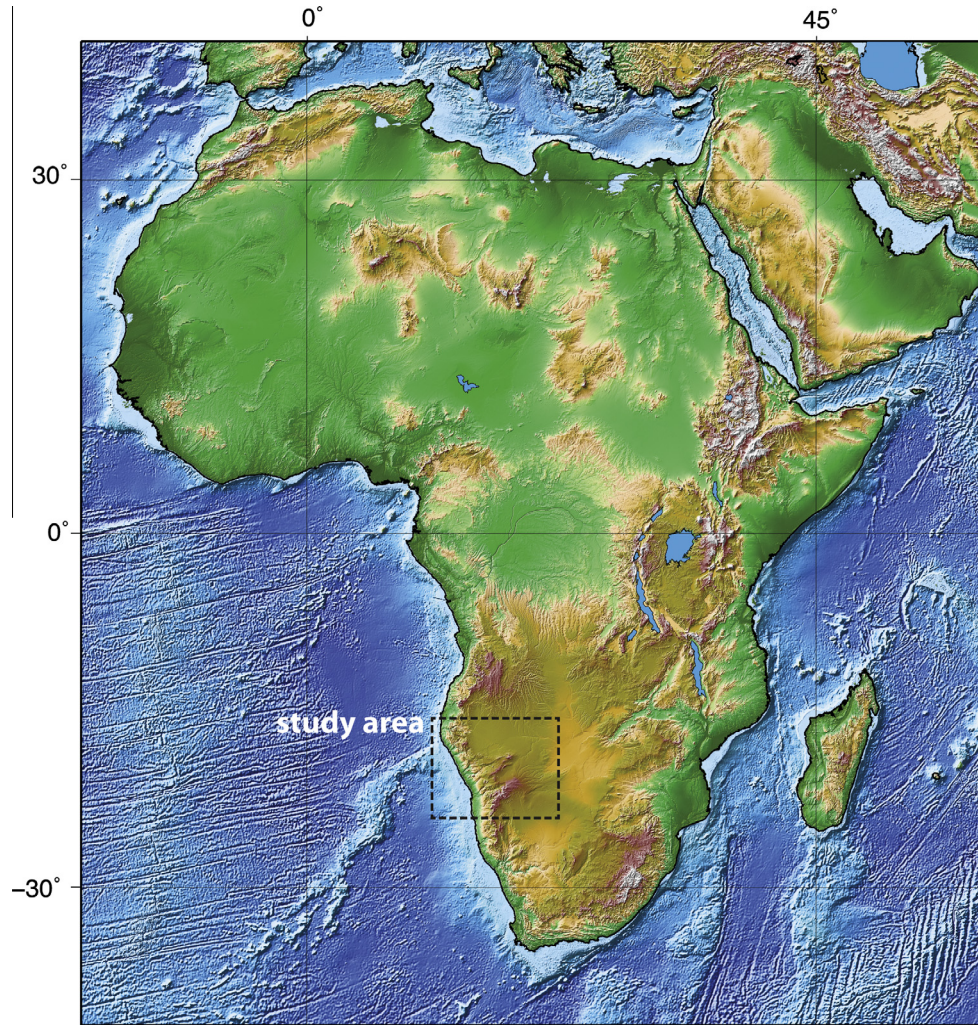


Fig. 1. Location of the study area within Africa. Shaded relief digital elevation image of Africa showing the location of the study area and its relationship to the regionally high topography of southern Africa. Note the prominent NE–SW trending structure of the topographic relief of the study area in northern Namibia. The topography is taken from the SRTM30Plus 1 km data (http://topex.ucsd.edu/WWW_html/srtm30_plus.html).

Damara metamorphic belt (Tankard et al., 1982; Martin and Eder, 1983; Miller, 1983) which forms part of the interconnected system of the ~500 Ma Pannotios (Stump, 1992) (Pan African of Africa, Delamarian of Australia, Ross of Antarctica, Brasiliano of South America) mobile belts which surround many of the cratonic terrains within Africa (Fig. 2) (Kennedy, 1964; Barton and Key, 1981; Kröner, 1977; Daly et al., 1989; Kampunzu et al., 1991; Light, 1982). The Damara metamorphic belt consists of two lithologically and structurally continuous branches; a 400–500 km wide intracontinental branch which trends NE-SW which separates the composite Zaire and Kalahari cratonic terrains, and a coastal branch which parallels the present Atlantic margin, trending NNW-SSE. The intracontinental branch of the Damara metamorphic belt forms the westerly extension of the Precambrian trans-continental Mwembeshi shear zone (Coward and Daly, 1984) has had a profound influence on the Phanerozoic geological history of central and southern Africa (e.g. Castaing, 1991; Daly et al., 1989, 1991; Maurin and Guiraud, 1993; Ring et al., 2002). The site and geometry of continental rifting, and the associated Etendeka magmatism, leading ultimately to the opening of the South Atlantic Ocean basin, appears also to have been influenced by the pre-existing crustal structure (e.g. Erlank, 1984; Porada, 1989). These intracontinental structures apparently also determined the location of many of the major oceanic transform faults and resultant fracture zones (Le Pichon and Fox, 1971; Fuller, 1971, 1972; Francheteau and Le Pichon, 1972; Sykes, 1978), as well as the locus of alkaline magmatism in southern Africa and southeastern Brazil (Marsh, 1973; Moore, 1976).

Most pre-rift plate reconstructions for South America and Africa (Rabinowitz and La Brecque, 1979; Keith Martin et al., 1981;

Martin, 1984, 1987; O'Connor and Duncan, 1990; Nürnberg and Müller, 1991; O'Connor and le Roex, 1992; Torsvik et al., 2009; Aslanian et al., 2009; Aslanian and Moulin, 2012) place northern Namibia within the predicted region of influence of the Tristan da Cunha mantle plume during the Early Cretaceous. Lithospheric extension and thinning over this region of anomalously hot mantle has been invoked as the cause of the Paraná-Etendeka flood basalt province (White and McKenzie, 1989; Peate et al., 1990; Marsh et al., 2001). Also, present seismic activity within southern Africa suggests that the Mwembeshi shear zone is currently tectonically active (Reeves, 1972, 1978; Reeves and Hutchins, 1975; Fairhead and Henderson, 1977; Daly et al., 1989), and recent tectonic reactivation along this structure is also indicated by ongoing active faulting which cuts Neogene dune sediments within the Okavango Graben in northern Botswana (Modisi, 2000; Modisi et al., 2000; Kinabo et al., 2007, 2008; Bufford et al., 2012).

There is some geological evidence for Late Mesozoic tectonism within northwestern Namibia that post dates the Etendeka volcanic episode. An occurrence of an easterly dipping sedimentary unit containing fining upward cycles of conglomeratic units comprised entirely of detritus derived from the Etendeka volcanics and preserving sedimentary structures indicating a westerly source region was documented by Ward and Martin (1987). They suggested that the unit represents syntectonic proximal deposition against a westerly dipping normal fault and proposed an early Cretaceous depositional age. Along the coastal region there are several NNW-SSE trending, westerly dipping normal faults which have displaced Etendeka lavas against basement to the east (down to the west displacement). The age of faulting is clearly post-Etendeka (post-Early Cretaceous) in both cases but there is no evidence

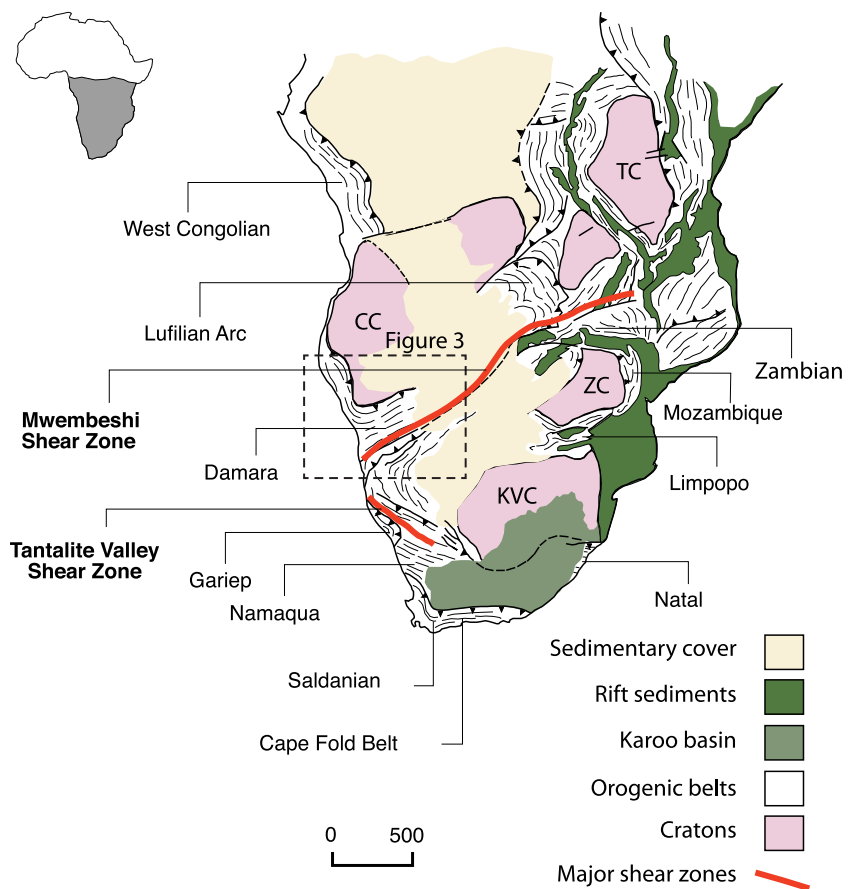


Fig. 2. Simplified map illustrating the basement tectonic framework of southern Africa. Note the strong NE-SW tectonic fabric in the study area and the major lithospheric scale shear zone systems. KVC, Kaapvaal craton; CC, Congo craton; TC, Tanzanian craton; ZC, Zimbabwe craton.

which provides a definitive lower age. However, seismic reflection data from the offshore Orange basin, further to the south, have shown that the Upper Cretaceous sedimentary sequence is strongly deformed on a regional scale (e.g. Dingle et al., 1983; de Vera et al., 2010).

2.2. Regional geology

The rocks of the Damaran Supergroup, forming the Damara orogeny and which dominate the present surface geology of north-western Namibia (Fig. 3), are comprised mainly of metasediments representing a sedimentary sequence deposited initially within narrow fault bounded depocenters. These sediments were subsequently overlain by a succession comprising platform carbonates followed by molasse-type clastic sediments in the north and a thick (>10 km) flysch-type succession within the Khomas trough to the south (Tankard et al., 1982; Martin and Eder, 1983). The sedimentary succession experienced regional metamorphism at high pressures and low temperatures (6–9 kb (18–27 km), <~450 °C; <~20 °C km⁻¹) along the southern margin of the intracontinental branch. Within the central Damara orogen contact metamorphism at low pressures and high temperatures (~2.5 kb (8–10 km), >~600 °C; ~70 °C km⁻¹) is also associated with voluminous granite plutonism (Martin and Eder, 1983; Miller, 1983). The regional metamorphic grade and the intensity of deformation rapidly diminishes northwards of the southern margin of the Kamanjab inlier.

Rb-Sr whole rock isochron ages from some of the granites and K-Ar and ⁴⁰Ar-³⁹Ar ages of metamorphic biotite and muscovite indicates cooling of the basement rocks, following the Pan-African orogenic phase, through ~300–350 °C between 545–480 Ma (e.g. Haack, 1983; Gray et al., 2006). Radiometric ages of the pre-Damara basement gneisses and metamorphosed supracrustal rocks indicate at least two prior periods of tectonism at ~2000 Ma (Eburnian/Ubendian) and between ~1400 Ma and

~900 Ma (Kibaran) (Porada, 1979) which are recognised elsewhere in Africa (Kröner, 1977; Hunter, 1981) and in South America where these two tectonic episodes are called the Transamazonian and the Uruacuano, respectively (Almeida et al., 1976; Cordani et al., 1973).

The nature of the tectonic setting of the intracontinental branch of the Damara metamorphic belt has been debated for many years (see reviews by Tankard et al. (1982) and Martin and Eder, (1983)). The arguments have largely revolved around the degree of plate divergence between the Zaire cratonic terrain to the north and the Kalahari cratonic terrain to the south, prior to plate convergence and the associated compressional deformation. Some models have proposed an active plate margin setting involving closure of a mature ocean basin resulting in continental collision with southward subduction of the Zaire cratonic plate beneath the Kalahari cratonic plate (Watters, 1976) while others have suggested similar models with the opposite subduction direction (Hartnady, 1974, 1979; Barnes and Sawyer, 1980; Kukla and Stanistreet, 1991). An alternative series of models envisage an entirely intracontinental rift setting with only minor plate divergence occurring prior to compressional deformation (Martin and Porada, 1977a, 1977b; Kröner, 1977, 1980; Martin, 1976; Porada, 1979; Henry et al., 1990). However, despite their variability all the tectonic models proposed for the Damara metamorphic belt agree that the NE-SW trending intracontinental branch represents a major tectonic boundary extending well into the sub-continental lithosphere, and that the initial lithospheric extension and rifting was followed by compression and shortening. This is supported by recent seismic tomography models of the African lithosphere (Fishwick and Bastow, 2011; Priestley et al., 2008).

The major tectonic boundaries within the intracontinental branch form regional lineaments (e.g. Okahandja, Omaruru and Us Pass lineaments) which delineate the NE-SW structural trend of the belt (Miller, 1979; Downing and Coward, 1981; Henry et al., 1990; Kukla and Stanistreet, 1991) (Fig. 3). The orientation of these lineaments reflects the regional structural trends that

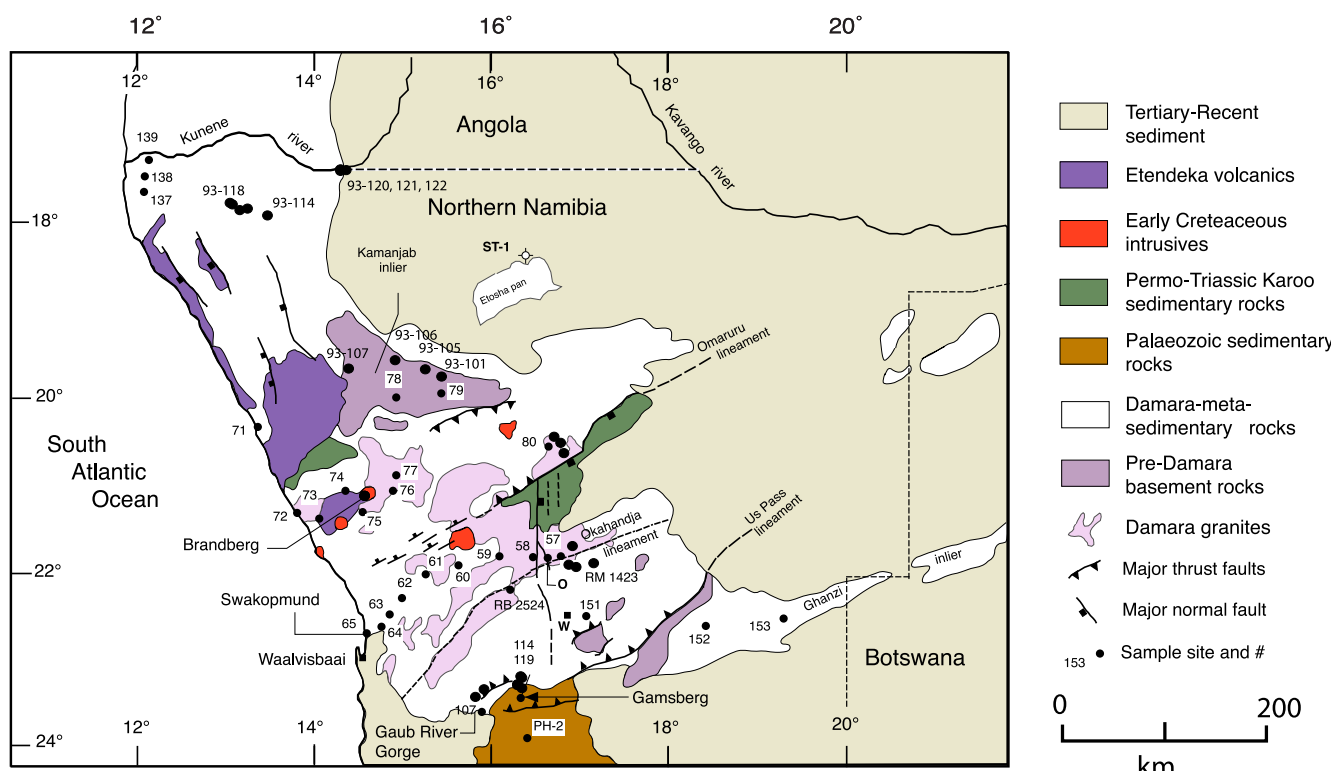


Fig. 3. Simplified geological map of northern Namibia. The geology is from the 1:4,000,000 geological sheet published by the Geological Society of South Africa (Hammerbeck and Allcock, 1985). Sample locations are shown on the map as black circles with the sample numbers indicated. W, Windhoek; O, Okahandja.

existed in the pre-Damara metamorphic basement which appear to have controlled the location of the rift basins into which the early Damara sediments were deposited (Tankard et al., 1982; Martin and Eder, 1983; Miller, 1983). This pattern of polyphase or superimposed Precambrian tectonism occurring within narrow zones or belts which separate more stable cratonic terrains is typical of the tectonic configuration of continental crust (De Swardt et al., 1965; Bois et al., 1990; Dallmeyer, 1990; Dallmeyer and Lecorche, 1990) and is particularly well documented in southern Africa (Tankard et al., 1982; Hunter, 1981; Kröner, 1977). This Precambrian tectonic framework continued to influence the geological development of northern Namibia throughout the Phanerozoic (e.g. Gevers, 1936; Clemson et al., 1997; Holzförster et al., 1999).

The basement is covered in parts by younger sedimentary sequences. Jurassic–early Cretaceous sediments occur beneath the cover of the Etendeka flood basalts (Jerram et al., 1999, 2000) and older Permo-Triassic sedimentary rocks occur in an outlier bounded to the north by a NE–SW trending high angle thrust (reverse?) fault (Holzförster et al., 1999). Conglomeratic units containing sub-rounded granitic pebbles and boulders which locally reach thicknesses of 17 m occur towards the base of the 600 m sequence. These coarse clastic basal layers suggest that the sediments were derived from a proximal basement source and were probably deposited within a fault bounded rift basin (Holzförster et al., 1999). Elsewhere in Africa the occurrence of Permo-Triassic (Karoo) sediments is also largely restricted to fault bounded inliers within the Precambrian metamorphic mobile belts (Fig. 2) (Rosendhal, 1987; Daly et al., 1989; Wopfner, 1988). Syntectonic deposition within fault bounded depocentres, commonly superimposed on older basement structures, is typical of many Gondwana Permo-Triassic basins (Cox et al., 1965; Green et al., 1980; Basu and Shrivastava, 1981; Wopfner, 1988; Nichols and Daly, 1989; Wopfner and Kaaya, 1991; Fielding and Webb, 1996). Sedimentation within the main Karoo basin of South Africa ended during the Late Triassic–Early Jurassic with a major phase of continental flood basalt volcanism (Eales et al., 1984) which foreshadowed the fragmentation of Gondwana. In contrast, sedimentation within northwestern Namibia appears to have continued until Early Cretaceous times (Dingle et al., 1983; Jerram et al., 1999, 2000) when it too was terminated by a major episode of flood basalt volcanism and accompanying sub-volcanic alkaline intrusives (Marsh, 1973; Moore, 1976; Erlank et al., 1984; Jerram et al., 1999), associated with the initial rifting leading to the opening of the South Atlantic. These volcanic rocks form the Etendeka volcanic province in Namibia (e.g. Erlank et al., 1984; Milner et al., 1995) and the Paraná flood basalt province in southeastern Brazil (e.g. Peate et al., 1990, 1997).

Radiometric ages for the Etendeka volcanics range from ~133 Ma to ~127 Ma (e.g. Trumbull et al., 2007). The oldest magnetic seafloor spreading anomaly recognised off the Namibian coast is anomaly M4 (~127 Ma) (Austin and Uchupi, 1982) while just north of the Falkland Agulhas Fracture Zone (FAFZ) the oldest magnetic anomaly identified is M11 (~133 Ma) (Martin, 1987; Cande et al., 1988) with successively younger anomalies abutting the continent ocean boundary in a northerly direction. The sub-aerial, post-Etendeka geology of northern Namibia is limited to a relatively thin (few hundred metres) and poorly dated Cenozoic sedimentary succession (Ward, 1987, 1988; Ward and Martin, 1987) and minor occurrences of alkaline volcanics (Auas Mountains, Windhoek) (Tankard et al., 1982; Marsh, 2010). Despite their limited extent these Cenozoic rocks provide information of considerable importance for understanding the post-Gondwana geological development of the region. The basal unit of the succession is the Tsondab Sandstone Formation believed to be of Early to Middle Tertiary in age (Ward, 1988) and which unconformably overlies an extensive erosion surface (Namib Unconformity Surface) cut into

the predominantly Late Precambrian basement rocks (Ollier, 1977, 1978; Ward, 1987, 1988). The Tsondab Sandstone Formation is comprised predominantly of reddish brown, quartz arenite and was deposited largely as desert dunes and sand sheets under arid conditions (Ward, 1987; 1988). The Karpenkliff Conglomerate Formation of probable Early Miocene age (Ward, 1987) unconformably overlies the Tsondab sandstone formation, and was deposited as large alluvial fans which wedge out westwards away from the foot of a major erosional escarpment cut into the Late Precambrian basement rocks. The alluvial nature of the Karpenkliff Conglomerate Formation and the assemblage of large (up to 95 cm), rounded to well rounded clasts of resistant rock types derived from the Precambrian basement implies substantial denudation of the escarpment region (Ward, 1987) at the time of deposition. The fluvial character and mode of deposition of this rudaceous deposit was interpreted by Ward (1987) as representing the earliest record of a well developed westerly directed drainage system and therefore a change from arid to semi-arid conditions. With the establishment in the Late Miocene of the cold, upwelling system of the Benguela Current there was a return to arid conditions which developed into the current Namib Desert regime (Siesser, 1978, 1980) promoting the accumulation of the Sossus Sand Formation which now forms the main Namib Sand Sea south of the Kuiseb river (Ward, 1987). Deep incision of the westerly directed Kuiseb drainage system since the Pliocene was interpreted by Ward (1987) as evidence for Late Tertiary epeirogenic uplift.

The regional topography of northern Namibia is dominated to the south by a prominent erosional escarpment cut into the Late Precambrian metamorphic or igneous rocks which runs sub-parallel to and between 100 km and 80 km from the present coastline (Ollier, 1977, 1978; Ward, 1987). At about 23° S the escarpment is cut by the Swakop river valley which has a northeasterly trend and runs roughly parallel to the Okahandja lineament and forms the northern boundary of the elevated region (> ~1400 m) known as the Khomas Hochland (Highland) which continues inland to become the Windhoek highlands. North of the Swakop river valley the escarpment diminishes to a graded surface which rises steadily eastwards from sea level at the coast to an elevated plateau (at 1400 ± 100 m) approximately 200–300 km inland. Numerous inselbergs occur seaward of the escarpment region and many of the Early Cretaceous alkaline intrusive rocks form isolated but spectacular mountains such as the Brandberg (2585 m), Erongo and Spitzkoppe.

There is clearly abundant geological and geophysical evidence for distinct, superimposed episodes of transcontinental intraplate tectonism in Africa. The Precambrian Ubendian (~2000 Ma) and Kibaran (~1100 Ma) episodes, the Pan-African episode during the earliest Phanerozoic (~500 Ma) and the Karoo episode during the Permo-Triassic (~230 Ma) and the Late Mesozoic episodes associated with the fragmentation of Gondwana and the development of the present ocean basins. This suggests that broadly coeval and spatially superimposed episodes of transcontinental tectonism are an integral part of continental dynamics, reflecting a fundamental and long-lived lithospheric structural configuration inherited from the earliest phases of continental assembly. Considering the past tectonic history of the Damara metamorphic belt it seems reasonable to expect the occurrence of discreet episodes of post-Gondwana tectonism, possibly coeval with episodes elsewhere in Africa, within northwestern Namibia.

3. Apatite fission track analysis results

The 38 rock samples analysed were collected from outcropping Damaran granites or metasediments, or from the pre-Damaran metamorphic basement rocks. The samples were collected over a

range of elevations from sea level up to 2260 m. Sample locations are indicated on the simplified geological map shown in Fig. 3. Details of the lithology of each sample are provided in Appendix 1. The sampling rationale was to collect a regional suite of Late Precambrian (pre-Karoo) samples over the maximum possible range of topographic elevations while being mindful of the regional structural and tectonic boundaries (such as the Omaruru and Okahandja lineaments). Within the central zone of the Damara belt a roughly NE–SW transect was sampled between Okahandja (~1450 m) and Swakopmund (sea level) over a horizontal distance of ~300 km. To the south of the Okahandja lineament, within the southern marginal zone, a ~1500 m vertical topographic profile was sampled over a horizontal distance of ~150 km between the Gaub river gorge (700 m) and Gamsberg (2260 m).

Apatite fission track ages and confined track length measurement results are reported for all samples in Table 1. Ages were measured by the external detector method (EDM) (Gleadow, 1981) using the zeta calibration technique (Hurford and Green, 1983; Green, 1985).

The apatite fission track ages measured for this study range from 59 ± 3 Ma to 449 ± 20 Ma, which closely matches the range determined by Haack (1976, 1983), Raab (2001) and Raab et al. (2002, 2005). Mean confined track length measurements range from 14.61 ± 0.20 μm to 10.83 ± 0.66 μm with the younger samples generally having the longer mean track lengths. There is a distinct lack of apatite fission track ages older than ~150 Ma at elevations below ~1000 m but ages younger than this occur below as well as above this elevation (Fig. 4). When all the apatite fission track ages are plotted against their distance north and south of, and measured perpendicular to, the Okahandja lineament a pattern remarkably similar to the age versus elevation plot is obtained (with distance substituting for elevation) (Fig. 4).

This relationship indicates a positive correlation between elevation and distance north and south of the Okahandja lineament, with generally lower elevations occurring to the north and higher elevations to the south (Fig. 4). This topographic relationship is clearly related to the development of the Swakop river valley which closely follows the NE–SW trend of the Okahandja lineament. This relationship suggests that the apatite fission track ages are correlated primarily with elevation, which is reflecting the possible influence of the Okahandja lineament on the location of the Swakop river valley. Apatite fission track ages also generally decrease towards the coast, reflecting the regional topography which is characterised by an elevated interior plateau separated from the coastal region by an escarpment south of the Swakop river but descending more gradually to sea level north of the Swakop river valley. Note that the ages for samples 8732-78 and 8732-79, of 437 ± 23 Ma and 435 ± 34 Ma respectively, are not shown in Fig. 4.

4. Discussion and interpretation of fission track results

Radiometric ages (summarised above) representative of the rocks sampled for apatite fission track analysis indicate that the present land surface exposes rocks that cooled to below ~300 °C (approximate closure temperature for K–Ar and ^{40}Ar – ^{39}Ar biotite ages) by ~480 Ma (Haack, 1976, 1983; Gray et al., 2006). In the northern coastal region there are several outliers of Permian glacial sediments preserved within pre-glacial valleys, cut by a westerly directed drainage system into the Late Precambrian basement rocks (Martin, 1953, 1976; Dingle et al., 1983; Visser, 1987). Isolated patches of glacial sediments also occur further south within the central Damara metamorphic belt. These glacial deposits suggest that the present land surface represents an exhumed pre-Permian erosion surface at some localities, or at least that the pres-

ent level of denudation has cut a new erosion surface at a level close to the Permian glacial surface. This would imply that many of the presently outcropping basement rocks were at, or close to, the surface before or at least by the end of the Permian glaciation. Some of the samples collected for apatite fission track analysis are therefore likely to have initially cooled to below $\sim 110 \pm 10$ °C at some time between ~500 Ma and ~260 Ma. The older apatite fission track ages of ~450 Ma confirms that some of the presently outcropping basement rocks did cool to below $\sim 110 \pm 10$ °C soon after the peak of Damaran orogenic activity at ~500 Ma and have since remained below this temperature.

Considering the regional structural features of the Damara metamorphic belt and the evidence for subsequent reactivation of many of them, it seems useful to examine separately the detail of AFTA results from within recognised structural domains. The eleven samples from the transect between Okahandja and Swakopmund (RM 1423 and 8732-57–8732-65) are bounded by the Okahandja lineament to the south and the Omaruru lineament to the north (Fig. 3) and are therefore considered as representative of that structural domain. The eight samples (RB 2543 and 8832-107–8832-119) making up the vertical topographic profile between the Gaub river gorge and the summit of Gamsberg are also considered to be representative of a single structural domain. The AFTA results for these two sample groups will be discussed in some detail and the conclusions drawn from this discussion will then be used as basis for interpreting the results obtained for the remaining samples.

4.1. Okahandja–Swakopmund transect

The apatite fission track ages from the Okahandja–Swakopmund transect decrease towards the coast from 449 ± 20 Ma ~40 km west of Okahandja (RM1423) to 69 ± 6 Ma (8732-62B) ~100 km east of Swakopmund. The three samples nearest the coast (8732-63, -64 and -65) gave slightly higher apatite fission track ages of $\sim 77 \pm 8$ Ma. Mean confined track lengths for the younger samples (<~80 Ma) range from 13.75 ± 0.18 μm to 14.61 ± 0.2 μm with an average value of ~14.2 μm . The samples with apatite fission track ages older than ~80 Ma have shorter mean confined track lengths which range from 14.18 ± 0.24 μm to 11.16 ± 0.70 μm . When the apatite fission track age and mean confined track length for each sample is plotted against sample elevation (Fig. 5) a pronounced inflection is apparent at ~1200 m on both the apatite age and the mean confined track length profiles. The apatite fission track ages remain relatively constant $\sim 75 \pm 5$ Ma from sea level up to ~1200 m and become rapidly older at higher elevations while the mean confined track length also remains relatively constant at ~14.2 μm up to the same threshold elevation but decreases rapidly above this elevation.

Single grain ages and confined track length distributions for a representative suite of samples from the Okahandja–Swakopmund transect are illustrated in Fig. 6. The composite radial plot (Galbraith, 1988, 1990) of the single grain ages (Fig. 6a), indicates a continuous array of ages from ~500 Ma through to ~70 Ma. The oldest sample, (RM1423) with a pooled age of 449 ± 40 Ma, and the youngest sample (8732-60A), with a pooled age of 71 ± 5 Ma, have no single grain ages significantly older or younger than their weighted mean grain ages (pooled ages). However, the two samples with intermediate apatite fission track ages (8732-57 and 8732-58) show a significant spread in single grain age but with all the apatite grains giving ages <~500 Ma and >~70 Ma. This difference in the distribution of single grain ages is clearly reflected by the c^2 statistic (Galbraith, 1981) for each sample which provides a measure of the dispersion or spread of single grain ages. The c^2 probabilities for both the oldest (RM1423; $P(\chi^2) = 69\%$) and youngest (8732-60A; $P(\chi^2) = 50\%$) samples indicates that the measured

Table 1

Apatite fission track data summary.

Sample#	Longitude	Latitude	Elevation (m)	NC	RhoS ($\times 10^6 \text{ cm}^{-1}$)	NS	Rhol ($\times 10^6 \text{ cm}^{-1}$)	NI	$P(\chi^2)$ (%)	RhoD ($\times 10^6 \text{ cm}^{-1}$)	ND	Age (Ma)	$\pm 1\sigma$	MTL (μm)	$\pm 1\sigma$	Std Dev (μm)	NL
8732-57	16.833	-21.967	1400	20	3.478	3271	4.514	4245	0	1.172	5152	164	± 8	11.16	± 0.35	3.52	100
8732-58	16.500	-21.950	1400	20	1.846	1267	4.049	2779	1.4	1.172	5152	95	± 5	12.16	± 0.31	3.22	100
8732-59 ^a	16.167	-21.967	1350	20	1.573	1702	3.644	3942	0	1.172	5152	92	± 6	11.18	± 0.37	3.68	100
8732-60 ^a	15.633	-21.967	900	19	1.605	1508	4.605	4326	45.8	1.172	5152	71	± 3	13.78	± 0.16	1.59	100
8732-61 ^a	15.200	-22.033	1070	19	1.537	1521	4.608	4560	2.2	1.172	5152	70	± 4	14.41	± 0.11	1.12	100
8732-62	15.050	-22.283	730	11	3.076	1083	9.094	3211	0.2	1.172	5152	70	± 4	14.48	± 0.31	1.41	21
8732-63	14.850	-22.500	420	20	2.156	1830	5.606	4757	0.1	1.172	5152	79	± 3	14.61	± 0.10	0.95	100
8732-64	14.750	-22.583	200	18	1.762	1358	9.182	7077	10.4	2.344	9958	78	± 3	13.75	± 0.09	0.96	110
8732-65	14.517	-22.633	20	10	2.411	501	6.458	1342	71.1	1.172	5152	76	± 4	14.36	± 0.12	1.17	100
8732-71	13.250	-20.250	10	20	1.108	1621	2.25	3290	34.2	1.296	12343	111	± 4	13.36	± 0.13	1.32	110
8732-72	13.667	-21.167	0	20	0.651	1172	1.359	2446	18.3	1.296	12343	108	± 4	13.44	± 0.16	1.62	105
8732-73	13.967	-21.417	140	15	1.031	762	2.516	1859	28.1	1.295	5435	92	± 4	13.68	± 0.17	1.09	40
8732-74	14.083	-21.083	440	20	1.148	2039	2.816	5003	81.2	1.296	12343	92	± 3	13.04	± 0.16	1.59	105
8732-75	14.500	-21.333	660	20	0.631	1179	1.411	2637	0.7	1.296	12343	102	± 6	12.87	± 0.20	2.06	103
8732-76 ^a	14.833	-21.067	790	21	1.103	1355	3.062	3761	3.6	1.296	12343	82	± 4	13.00	± 0.18	1.86	105
8732-77 ^a	15.000	-20.950	700	20	1.373	2075	4.001	6046	2.5	1.296	12343	82	± 3	12.65	± 0.17	1.92	130
8732-78 ^a	15.050	-20.083	1180	20	1.838	1272	0.922	638	76.8	1.295	5435	437	± 23	12.10	± 0.21	1.75	69
8732-79 ^a	15.467	-20.050	1250	15	2.193	1294	1.144	675	1.5	1.295	5435	435	± 34	11.71	± 0.22	1.74	60
8732-80	16.667	-20.500	1570	20	0.201	1498	8.831	6573	0.3	2.344	9958	92	± 4	13.49	± 0.16	1.64	104
8832-107 ^a	15.767	-23.467	740	20	0.253	422	0.599	999	93.5	1.228	5540	90	± 6	14.39	± 0.29	1.03	13
8832-108 ^a	15.867	-23.383	1000	6	0.155	64	0.268	111	92	1.196	3125	120	± 19	–	–	–	–
8832-110 ^a	16.283	-23.233	1450	20	0.516	593	0.516	593	18.4	1.24	5540	214	± 13	12.01	± 0.25	2.48	99
8832-111 ^a	16.300	-23.250	1650	20	0.076	129	0.051	87	75.5	1.252	5540	317	± 44	13.48	± 0.43	1.59	14
8832-114 ^a	16.250	-23.333	2260	20	0.781	616	0.672	530	60.3	1.264	5540	252	± 16	12.00	± 0.40	2.09	27
8832-116 ^a	16.250	-23.325	2050	20	0.644	523	0.715	581	95.3	1.276	5540	198	± 13	12.10	± 0.21	2.07	100
8832-119 ^a	16.300	-23.367	1845	13	0.348	268	0.711	547	0.3	1.288	5540	159	± 21	–	–	–	–
8832-137	11.950	-17.667	100	20	0.505	888	1.124	1976	27.3	0.944	3145	74	± 3	14.59	± 0.18	1.31	54
8832-138	11.900	-17.350	100	20	0.786	1216	2.365	3660	5.4	0.963	3145	59	± 3	13.74	± 0.15	1.53	100
8832-139	12.017	-17.217	100	20	0.364	540	0.908	1346	82.6	0.983	3145	69	± 4	14.59	± 0.21	1.43	47
8832-151	17.183	-22.567	1770	6	0.331	113	0.304	104	68.8	0.983	4441	184	± 25	–	–	–	–
8832-152	18.950	-22.433	1470	6	0.294	52	0.232	41	96.3	0.985	4441	277	± 52	–	–	–	–
8832-153	19.783	-22.383	1330	20	1.64	1009	1.003	617	1.3	0.988	4441	289	± 21	12.44	± 0.22	1.38	40
MD-008	14.500	-21.180	1000	20	3.644	2863	7.664	6022	1	1.299	16176	111	± 9	13.68	± 0.12	1.24	115
MD-012	14.500	-21.180	1500	20	0.349	405	0.721	837	99	1.299	16176	109	± 14	13.94	± 0.44	2.16	24
MD-104	14.500	-21.180	650	24	0.446	374	1.185	9930	40	1.262	7331	83	± 5	13.42	± 0.3	1.78	34
PH-2 ^a	16.330	-23.800	1500	20	1.971	2555	1.529	1982	46.5	1.305	10780	288	± 12	11.92	± 0.19	1.78	92
RB 2543	15.530	-22.200	1125	20	0.726	1174	1.927	3115	18.1	1.281	10780	84	± 4	14.18	± 0.14	1.11	62
RM1423	17.117	-21.950	1450	10	3.079	1862	1.561	944	68.7	1.345	9996	449	± 20	11.40	± 0.2	2	100
93-099	16.917	-21.992	1310	19	0.614	619	0.504	508	10	1.171	6490	239	± 17	11.30	± 0.27	1.84	47
93-100	16.875	-21.757	1520	20	3.649	2529	2.843	1970	60	1.171	6490	250	± 8	10.94	± 0.26	2.62	100
93-101	16.780	-20.688	1620	16	2.045	615	3.993	1201	80	1.171	6490	101	± 5	12.44	± 0.16	1.62	101
93-104	16.788	-20.678	1600	20	1.298	1002	2.386	1842	75	1.171	6490	107	± 4	13.15	± 0.15	1.45	100
93-105	16.743	-20.573	1570	20	0.587	413	1.263	889	15	1.171	6490	91	± 6	13.68	± 0.14	1.4	102
93-106 ^a	15.380	-19.805	1240	20	2.35	1176	1.437	719	1	1.171	6490	329	± 27	11.86	± 0.16	1.65	101
93-107 ^a	15.195	-19.723	1190	20	1.535	932	0.926	562	75	1.171	6490	321	± 18	11.99	± 0.21	1.86	100
93-108 ^a	14.850	-19.617	1220	20	1.284	742	0.849	491	50	1.171	6490	293	± 18	12.49	± 0.30	1.21	102
93-110 ^a	14.318	-19.713	1190	20	2.54	1218	1.576	756	25	1.171	6490	311	± 16	11.43	± 0.25	1.84	103
93-114	13.392	-17.933	900	20	2.138	794	1.308	486	65	1.171	6490	315	± 19	11.94	± 0.24	1.68	50
93-115	13.167	-17.850	1080	16	2.347	680	1.381	400	40	1.171	6490	329	± 21	11.85	± 0.25	1.35	29
93-116	13.075	-17.867	1180	20	2.884	1439	1.91	953	20	1.171	6490	296	± 15	11.86	± 0.18	1.79	104
93-117	12.965	-17.782	1220	12	2.29	346	1.43	216	75	1.171	6490	310	± 27	11.60	± 0.25	1.38	31
93-118	12.992	-17.804	1250	20	0.942	577	0.553	339	80	1.171	6490	329	± 23	11.84	± 0.22	1.76	64
93-120	14.225	-17.392	940	20	2.435	1593	1.756	1149	80	1.171	6490	269	± 11	11.89	± 0.15	1.55	101
93-121	14.227	-17.408	850	20	2.678	1277	1.99	949	35	1.171	6490	262	± 13	11.38	± 0.16	1.6	100
93-122	14.290	-17.402	1180	7	3.447	516	2.198	329	4	1.171	6490	305	± 29	11.94	± 0.18	1.17	43
93-125	15.678	-24.671	712	12	0.322	95	0.762	225	75	1.171	6490	83	± 10	11.28	± 0.83	3.22	16

Ages calculated using a zeta calibration value of 350.2 ± 5 for NBS glass SRM 612. The mean crystal age is reported where $P(\chi^2) < 5\%$.93-XXX sample series ages calculated using dosimeter glass CN-5, analyst A. Carter CN5 Zeta = 339 ± 5 .

RhoS-measured spontaneous track density: NS-number of spontaneous tracks counted.

RhoL-measured induced track density: NI-number of induced tracks counted.

 $P(\chi^2)$ -probability of obtaining observed χ^2 value for n degrees of freedom ($v =$ number of crystals – 1).RhoD-track density measured in external detector adjacent to the glass dosimeter during irradiation. ND-number of tracks counted in determining ρd .MTL-mean confined track length ± 1 sigma standard error calculated for NL length measurements.

Std. Dev. – standard deviation of track length distribution of NL individual track measurements. NC = number of crystals.

Longitude and latitude coordinates are in decimal degrees relative to the WGS84 datum.

^{a</}

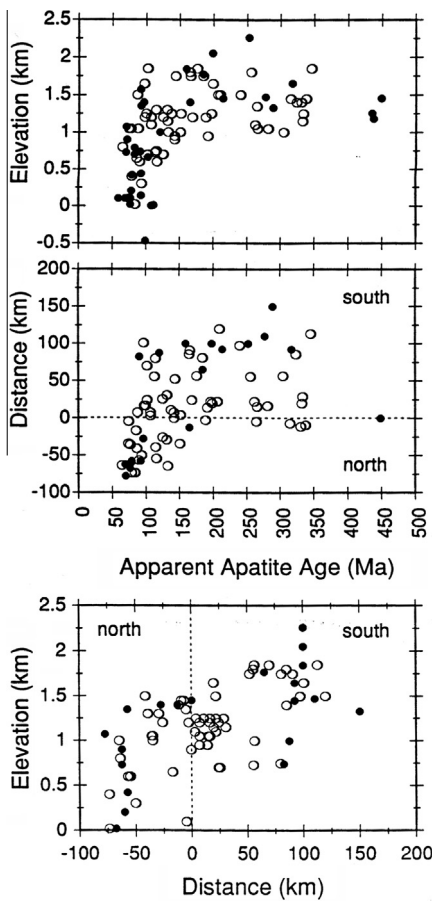


Fig. 4. Comparison between apatite fission track ages from this study (black circles, I) and those from Haack (1976, 1983) (open circles). In the two upper panels apatite fission track age is plotted against sample elevation and sample distance south (positive) or north (negative) of the Okahandja lineament (see Fig. 3). In the lower panel sample elevation is plotted against sample distance south (positive) or north (negative) of the Okahandja lineament. The similarity between the two distributions of apatite age, shown in the upper two panels, implies that there is a positive correlation between elevation and distance south (positive) of north the Okahandja lineament. This is relationship is confirmed by the positive correlation between sample elevation and distance south or north of the Okahandja Lineament shown in the lower panel. Apatite fission track age is therefore primarily correlated with elevation, which itself is correlated with distance from the Okahandja lineament. This pattern largely results from the coincidence between the Swakop River valley and the Okahandja lineament, and therefore does not necessarily imply any structural displacement across the lineament.

have experienced a range of post-Damara maximum palaeotemperatures prior to an episode of cooling at approximately 70 Ma, with the oldest sample having experienced only a moderate to low degree of thermal annealing since initially cooling to somewhat less than ~70 °C at or before ~500 Ma and with the youngest sample having experienced temperatures in excess of 110 ± 10 °C prior to ~70 Ma.

The confined track length distributions (Fig. 6a) for these samples provide additional support for the proposed interpretation of the apatite fission track ages. The youngest samples (8732-60A and 8732-61) both have narrow, unimodal confined track length distributions with mean track lengths of ~14 µm and standard deviations slightly greater than 1 µm. The older samples all have much broader track length distributions and shorter mean track lengths (11.20–12.16 µm), as a consequence of having a significant number of short tracks (<~10 µm) present in addition to a longer component of tracks similar to that preserved by the youngest samples. In the oldest sample (RM1423) the shorter tracks represent the major component of the distribution with a modal

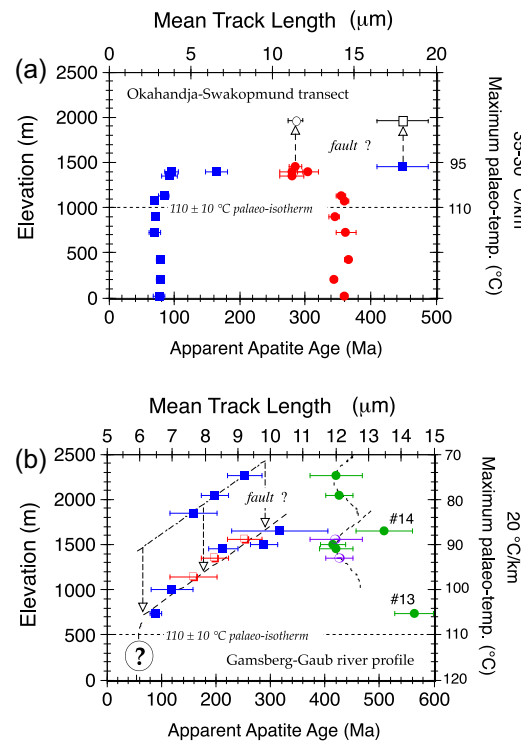


Fig. 5. Apatite fission track age (filled squares) and mean confined track length (filled circles) plotted against sample elevation for the samples from the Okahandja-Swakopmund transect (upper panel) and the Gamsberg-Gaub River profile (lower panel). The anticipated break-in-slope at an age of c. 80–70 Ma and elevation of c. 500 m is shown by the black dashed line and question mark symbol below c. 500 m on the Gamsberg-Gaub River age-elevation trajectory. This is based on extrapolation of the age-elevation relationship observed for the Okahandja-Swakopmund transect above. The maximum palaeotemperatures indicated by the scales on the right were estimated from the confined track length distributions and the degree of age reduction, assuming an initial age of ~500 Ma. These palaeotemperatures are not well constrained but they do suggest that relatively 'normal' palaeogeothermal gradients existed within the shallow crust prior to the initiation of denudation. The restored positions of samples that are believed to have been displaced by faults are shown on both diagrams by the open symbols (see text for discussion).

length between ~11 µm and ~12 µm, and the longer component of tracks forms a much smaller peak with a modal length of ~14 µm. As the apatite fission track age decreases so too does the modal length of the shorter component of fission tracks, but the modal length of the longer component remains at ~14 µm and it becomes the dominant modal length. Once the age has been reduced to the minimum age of ~70 Ma only the longer component of tracks remains.

This relationship between apatite fission track age and the detailed shape of the confined track length distributions is characteristic of a suite of samples that records various degrees of thermal annealing (thermal resetting of the apatite fission track age) which occurred prior to a common episode of cooling (e.g. Gallagher et al., 1998). The pronounced inflection in the apatite fission track age and mean confined track length profiles (Fig. 5) marks the transition from partially annealed samples (above the inflection) to completely annealed samples (below the inflection). This transition therefore represents the position of the 110 ± 10 °C palaeoisotherm (the maximum temperature for fission track retention in apatite) prior to cooling, implying that samples above this transition have experienced palaeotemperatures less than ~110 °C and those below the transition temperatures greater than ~110 °C. The age at which this inflection occurs will thus closely approximate the time at which cooling began.

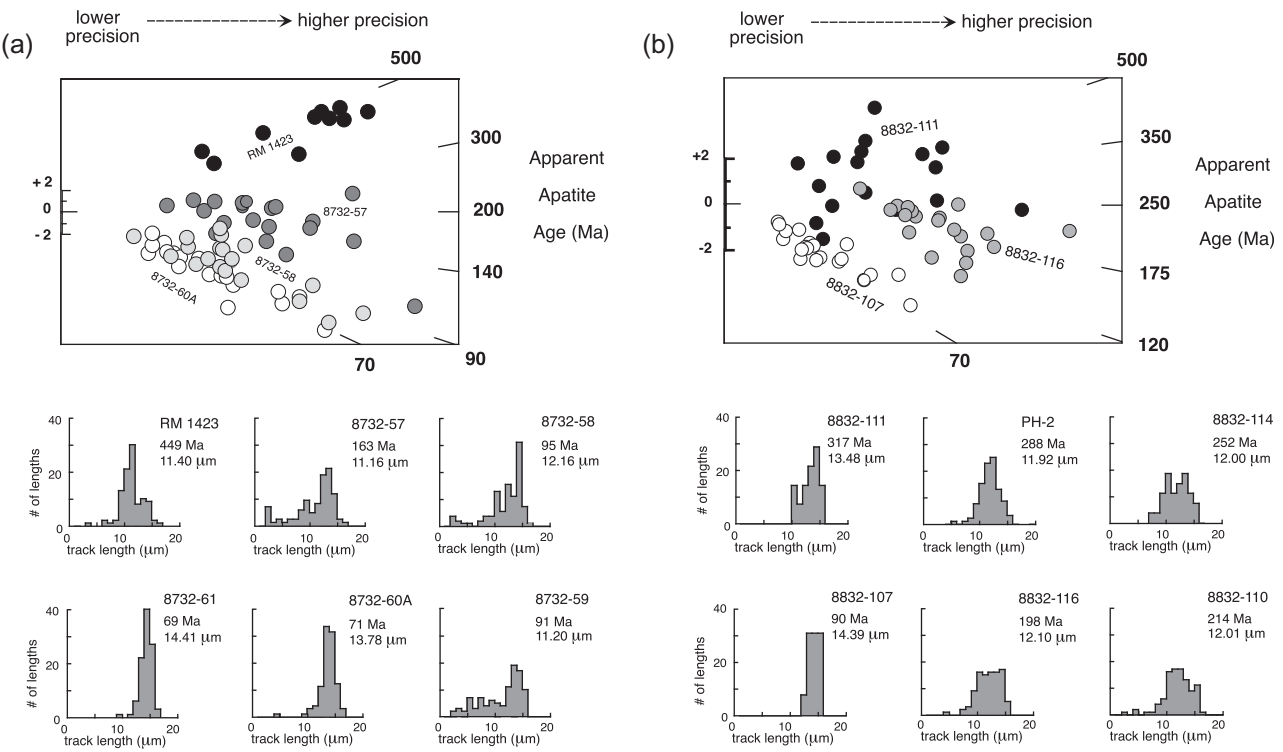


Fig. 6. Single grain ages, shown on a composite radial plot (Galbraith, 1988, 1990) and confined track length distributions for selected samples. (a) Samples from the Okahandja–Swakopmund transect. (b) Samples from the Gamsberg–Gaub River profile (see Appendix 1 for sample localities and text for detailed discussion).

4.2. Gamsberg–Gaub river profile

The eight apatite fission track ages from the Gamsberg–Gaub river profile range from 317 ± 44 Ma (8832-111) to 90 ± 6 Ma (8832-107). When apatite fission track age is plotted against sample elevation two essentially linear and parallel trends are apparent (Fig. 5), with the three highest samples forming one profile and the five lower samples forming the other. In both profiles the apatite fission track age is strongly correlated with elevation with a gradient of ~ 3 m Ma $^{-1}$. Apart for the oldest and the youngest samples (8832-111 and 8832-107) the mean confined track lengths are all similar and range from 11.92 ± 0.38 μm to 12.10 ± 0.42 μm. The mean lengths for both the oldest and the youngest sample are longer, 13.48 ± 0.86 μm and 14.39 ± 0.58 μm, respectively, but are likely to be biased towards longer lengths seeing that only a small number (<20) of tracks were measured for these samples.

Single grain ages and confined track length distributions for selected samples are illustrated in Fig. 6b. As for the Okahandja–Swakopmund transect samples the single grain ages form a continuous array between ~ 500 Ma and ~ 70 Ma. However, all the samples (except 8832-119) from the Gamsberg–Gaub river profile have χ^2 probabilities that indicate that the spread in single grain ages is consistent with each sample representing a single age population ($P(\chi^2) \geq \sim 5\%$). This may be due, in part at least, to the generally low precision of the single grain age estimates for these samples. This distribution of single grain ages suggests that these eight samples may also be reflecting a range of post-Damaran maximum palaeotemperatures prior to cooling during the Late Cretaceous.

This interpretation is supported by the confined track length measurements for these samples. Despite having similar mean confined track lengths, the confined track length distributions for the four intermediate age samples shown in Fig. 6b have some important differences. Sample PH-2 has a distinctly unimodal but moderately wide (standard deviation of 1.78 μm) distribution of

confined track lengths with a mean length of 11.92 ± 0.38 μm and an apatite fission track age of 288 ± 24 Ma. Sample 8832-114 on the other hand has a slightly broader (standard deviation of 2.09 μm) confined track length distribution which appears to be bimodal and has a younger age of 252 ± 32 Ma. The confined track length distributions for samples 8832-110 and 8832-116, which have slightly younger ages of 214 ± 26 Ma and 198 ± 26 Ma respectively, are also broad (standard deviations of 2.48 μm and 2.07 μm) and do not appear to be unimodal. The youngest sample (8832-107) which has an age of 90 ± 12 Ma has an apparently unimodal and relatively narrow (standard deviation of 1.03 μm) confined track length distribution with a mean length of 14.39 ± 0.58 μm. However, seeing that only 13 confined tracks were measured for this sample (8832-107) the measurement is not very reliable. In spite of the uncertainty in the confined track length measurements the overall relationship between apatite fission track age and the shape of the track length distributions is similar to that shown by the samples from the Okahandja–Swakopmund transect.

The similarity in the apatite age-elevation gradient for both the upper and lower profiles (Fig. 5), in conjunction with the observation that all eight samples form an apparently coherent series reflecting various degrees of thermal annealing, suggests that the two profiles may simply represent displaced segments of the same profile. This would imply that the upper three samples are from a crustal block that has been displaced upwards, relative to the other samples, by approximately 700 m. The three highest samples (8832-119, 8832-116, 8832-114) were all collected from the Gamsberg two-mica granite and the other samples (except PH-2) were collected from Damaran micaceous schists. The Gamsberg granite is bounded to the north and south by thrust faults which form part of the southern boundary to the Damara metamorphic belt. It seems possible therefore that these faults have been reactivated in post-Damara times and that the Gamsberg is part of a crustal block that has been displaced upwards relative to the surrounding region. It is interesting to note that the summit of Gamsberg, which is the second highest peak (2326 m) in Namibia, is

capped by a thin (~10 m) layer of quartz cemented sandstone believed to be of late Karoo age (Triassic). This small outlier is the only occurrence of Karoo age sediments in this region (Dingle et al., 1983).

4.3. Etendeka–Brandberg region

The eight samples (8732-71 to 8732-77 and 8732-80) bounded to the south by the Omaruru lineament and to the north by the northern boundary of the Damara metamorphic belt form a distinct group with uniformly similar apatite fission track ages and confined track length distributions. The apatite fission track ages range from 81 ± 12 Ma to 110 ± 16 Ma with mean confined track lengths between 12.65 ± 0.34 μm and 13.49 ± 0.32 μm . The confined track length distributions are all unimodal with a modal length between ~13 and 14 μm and several samples (8732-74, 8732-75 and 8732-77) have subtle but distinct tails of highly annealed tracks (<~10 μm) which is reflected by the slightly higher standard deviations for these samples of between 1.59 μm and 2.06 μm . The distribution of single grain ages for the eight samples is variable with four of the samples having χ^2 probabilities <5% and four >5% with the older samples generally having the higher values. Most of the single grain ages (for all eight samples) range from an older limit of ~140 Ma to a lower limit of about ~70 Ma but the younger samples do have a few grains which are significantly younger than 70 Ma.

The distinctly unimodal and relatively narrow character of the confined track length distributions for samples with apatite fission track ages older than ~70 Ma and the paucity of highly annealed tracks (<~10 μm) within these distributions is markedly different from both the Okahandja–Swakopmund transect and the Gamsberg profile samples. This distinctive form of the confined track length distributions and the lack of any single grain ages much older than ~140 Ma suggests that all these samples were exposed to palaeotemperatures in excess of $\sim 110 \pm 10$ °C (and thus were completely annealed) during the earliest Cretaceous. The lower limit to the range of single grain ages of ~70 Ma (noting that there are also a few younger grains) suggests that, like the previous two sample suites, many of these samples remained at elevated temperatures ($\sim 100 \pm 10$ °C) until approximately 70 Ma. Also, the generally broad spread of single grain ages and the reduced modal track lengths of ~13 μm for most of these samples indicate that cooling from these elevated temperatures was probably protracted.

4.4. A regional framework for interpretation of the fission track results

A useful regional summary of the AFTA results for all samples north of and including the Okahandja–Swakopmund transect is provided by plotting apatite fission track age against the mean confined track length for each sample (Fig. 7). Selected confined track length distributions are also shown in Fig. 7 as are histograms of available radiometric ages for the Damaran metasediments and granites (Martin and Eder, 1983) and for the Etendeka volcanics and sub-volcanic intrusions (Marsh, 1973; Fitch and Miller, 1984; Trumbull et al., 2007). The AFTA parameters predicted by the thermal modelling results which are presented and discussed in the next section are also indicated on the diagrams of Fig. 7 (the open symbols).

The regional relationship between apatite fission track age and mean confined track length is clearly demonstrated in Fig. 7 which shows the youngest and oldest samples having the longer, and the intermediate age samples having the shorter, mean confined track lengths. This general pattern, sometimes referred to as a “boomerang trend”, is typical of a suite of samples representing various degrees of partial annealing with the apparent apatite fission track

ages for the various samples ranging between a common older initial age, and a younger terminal age which closely approximates the time that cooling from the maximum palaeotemperatures began. The oldest apatite fission track ages measured of ~450 Ma (RM 1423, 8732-78 and 8732-79) are younger but close to the peak of Damaran metamorphism and granite intrusion which is illustrated by the histogram of radiometric ages shown in Fig. 7a. However, the shortened mean track lengths (11.40 ± 0.4 μm to 12.10 ± 0.42 μm) and the distinct positive skewness of the distribution of track lengths for these samples indicates that they cooled to below $\sim 110 \pm 10$ °C some time before ~450 Ma. The presence of single grain ages of around ~500 Ma in these older samples also points towards initial cooling being somewhat earlier than ~450 Ma and thus closely following the peak of Damaran metamorphism and granite plutonism at ~500 Ma. The youngest samples with the longest mean track lengths suggest that a distinct episode of cooling began at ~70 Ma, which post-dates the Etendeka magmatism by at least 40 Ma. The regional AFTA data set thus appears to represent a boomerang-type trend with an apparent initial apatite fission track age of close of ~500 Ma and a younger terminal age of ~70 Ma.

Examining the cluster of AFTA data forming the younger end of the apparent regional boomerang trend at a more appropriate scale (Fig. 7b) reveals a more complicated relationship between apatite fission track age and mean confined track length. The samples from the Okahandja–Swakopmund transect appear to conform to the regional boomerang trend in that the mean track length decreases progressively as the apatite fission track age increases from the terminal age of ~70 Ma towards the apparent initial age of ~500 Ma. However, the samples from the Etendeka–Brandberg region clearly deviate from the apparent regional trend forming an array in which the mean confined track length actually increases as the apatite fission track age increases. The oldest apatite fission track age obtained from the basement samples from the Etendeka–Brandberg region is remarkably similar to the younger limit of Etendeka magmatism at close to 120 Ma and coincides with the older apatite fission track ages obtained for the Brandberg alkaline ring complex (samples MD 08 and MD 12). It is tempting, therefore, to suggest that this distinct secondary array forms a younger boomerang trend with an apparent initial age of about 110–120 Ma but with the same terminal age (~70 Ma) as the regional trend. This secondary array may be thought of as representing a “younger” boomerang trend which was initiated by thermal overprinting of the basement rocks during the Etendeka magmatic episode, and was terminated by the same cooling episode recorded by the regional or “older” boomerang trend at ~70 Ma.

In reality, the cluster of AFTA data shown in Fig. 7b occupies a roughly wedge shaped region bounded at the top by an idealised “younger” boomerang trend and at the bottom by the idealised “older” regional boomerang trend. This distribution of the AFTA data is to be expected if an “older” boomerang trend is only partially reset by a younger episode of thermal annealing. This scenario is illustrated schematically in Fig. 8. Imagine a sequence of samples which cooled instantaneously from temperatures greater than $\sim 110 \pm 10$ °C to a range of temperatures between 110 ± 10 °C and ~ 20 °C at ~500 Ma. If these samples subsequently remained at these temperatures until ~70 Ma at which time they all began to cool until they were all at ~20 °C by the present, then the apatite fission track ages and mean track lengths of these samples could be expected to form an idealistic boomerang trend such as the “Old Boomerang” shown in Fig. 8a.

Consider a hypothetical sample (solid black dots in Fig. 8a) shown as a member of this idealistic “Old Boomerang” trend. If this sample was subjected to elevated temperatures at ~120 Ma then all the fission tracks that had accumulated over the 380 million years since the sample first cooled below 110 ± 10 °C (that is

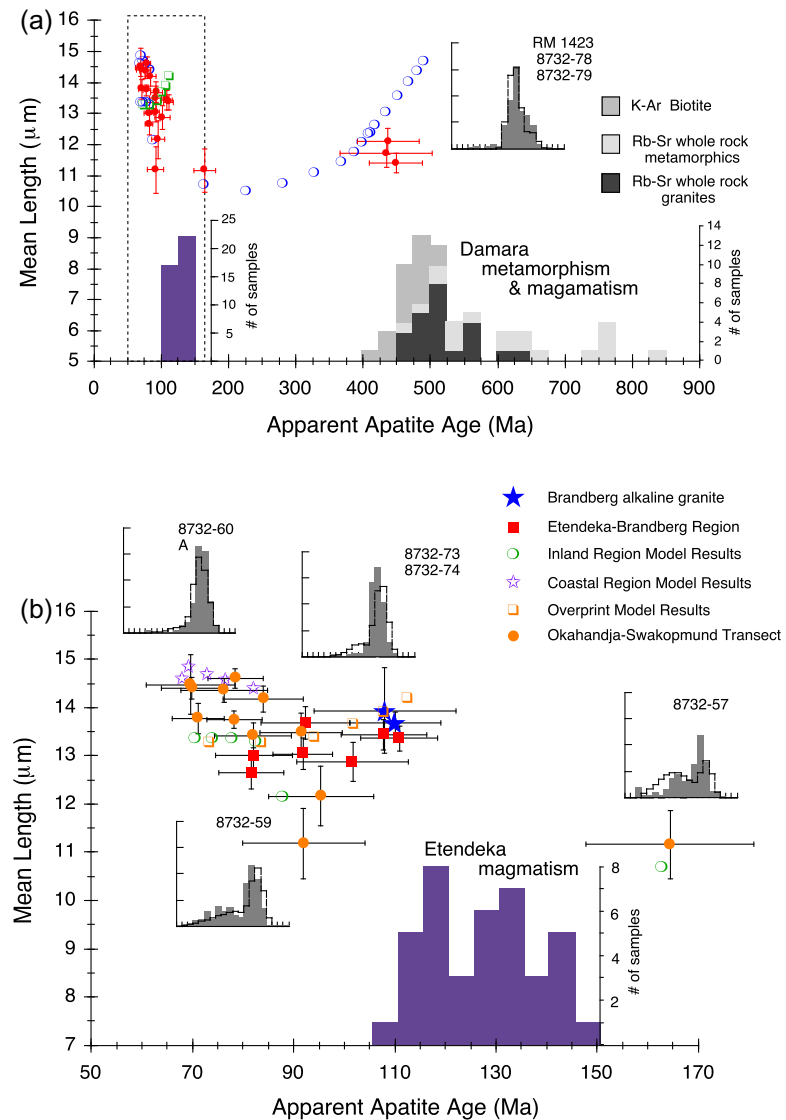


Fig. 7. 'Boomerang' plots of apatite fission track age against mean confined track length. Data shown are for all samples north of and including the Okahandja–Swakopmund transect samples (filled symbols) and the modelled AFTA results (open symbols). All the data are shown in a and a sub-set of the data (ages < 200 Ma) is shown at an expanded scale in b. The modelled AFTA parameters were generated by the thermal models discussed in the text and illustrated in Fig. 9 in conjunction with the annealing model of Laslett et al. (1987). The open squares represent results from the Overprint model (samples affected by the Etendeka magmatism), the open circles represent results from the Inland model and the open stars results from the Coastal model. Measured confined track length distributions for selected samples are also shown as shaded histograms, and are labelled accordingly. Modelled confined track length distributions (dashed black lines) are shown superimposed on the measured length distributions. The histograms shown along the base of the 'boomerang' plots were constructed using appropriate radiometric ages for the Damara metamorphic and granitic rocks (Martin and Eder, 1983), and for the Etendeka volcanic rocks (Marsh, 1973; Fitch and Miller, 1984; Trumbull et al., 2007).

~500 Ma) would be further annealed and thus become shorter. If the additional thermal annealing was sufficient to severely shorten the pre-existing fission tracks, such that their mean length was reduced to less than ~11–12 μm , they would represent a significantly smaller proportion of the final track length distribution. This would occur because of the highly biased nature of the track length measurements which are strongly biased towards track lengths greater than ~11 μm (Laslett et al., 1982). The long component of tracks which accumulated after cooling began at ~70 Ma would thus represent a greater proportion of the final distribution of confined track lengths and the mean length would be longer. The apparent fission track age, however, would be reduced because the earlier formed tracks (those that formed prior to thermal annealing) would contribute less to the final fission track age.

The resultant reduction in apparent fission track age and increase in mean confined track length for our hypothetical sample

causes it to shift its position on the boomerang plot towards longer mean lengths and younger ages (Fig. 8a). The degree of thermal annealing at ~120 Ma would determine the magnitude of this shift. If the increased temperature was sufficient to completely erase all the pre-existing fission tracks then the sample would move onto the "Young Boomerang" with its position on this new boomerang trend being a function of the degree of thermal annealing experienced between ~120 Ma and the initiation of the terminal cooling episode at ~70 Ma. The distribution of the AFTA data shown in Fig. 8b therefore suggests that the Etendeka–Brandberg samples may have been exposed to elevated temperatures during the Etendeka magmatic episode which were sufficient to cause severe, but generally not complete, thermal annealing of any pre-existing fission tracks.

Several qualitative, but nevertheless important, constraints can now be placed on the likely post-Damara thermal history of the

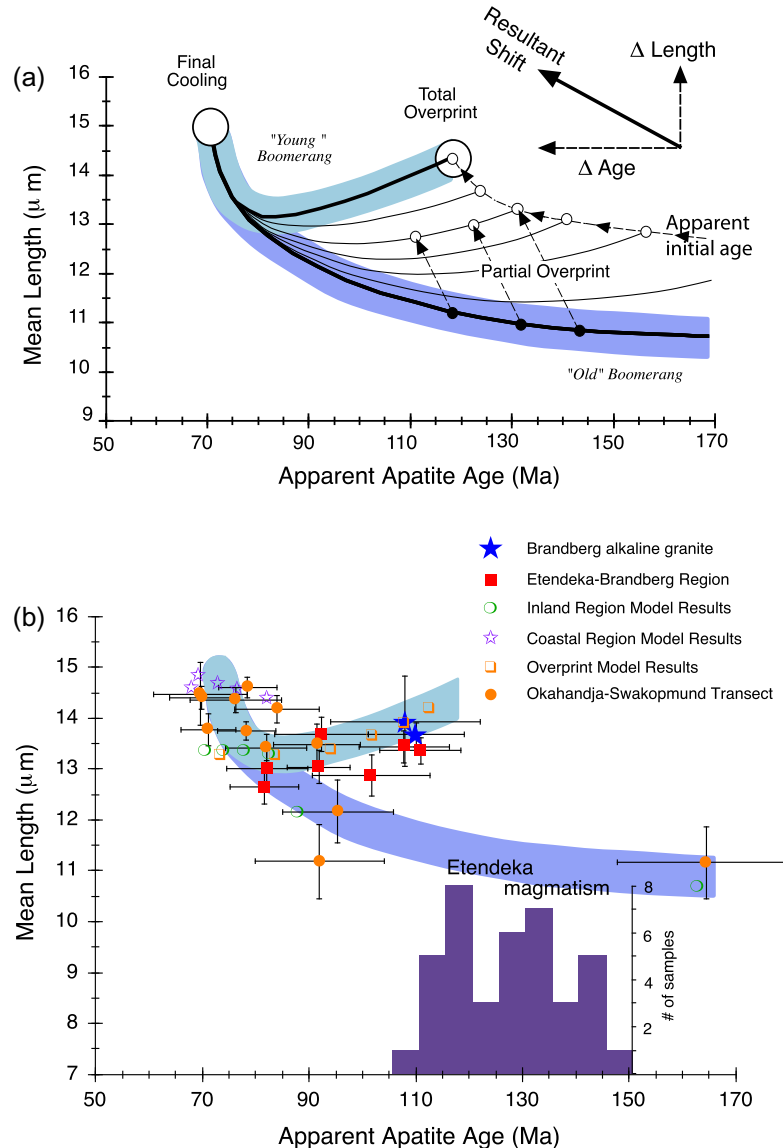


Fig. 8. (a) Schematic diagram illustrating the theoretical relationship between an idealised 'older' boomerang trend and a 'younger' boomerang trend, having different initial ages but the same terminal age (~70 Ma in this case). The idealised 'young' boomerang trend corresponds to the modelled AFTA results from the Overprint model and the 'old' boomerang corresponds to the results from the Inland model (the thermal models are discussed in the text). The trajectories of samples that are only partially annealed by the thermal event at ~120 Ma (Etendeka magmatism?) are illustrated by the dashed arrows. This shift, towards lower apparent apatite ages and longer mean confined track lengths, results from a reduction in the proportion of shortened tracks which contribute to both the age and mean length measurements. (b) Diagrammatic summary of the relationship between the measured AFTA data and the theoretical, end member, boomerang models.

presently outcropping basement rocks of northern Namibia. The maximum palaeotemperatures experienced by most of these rocks since initial post-Damara cooling must have been less than $110 \pm 10^\circ\text{C}$ except for those samples with apatite fission track ages of ~70 Ma or younger. However, some samples may have been exposed to temperatures in excess of $110 \pm 10^\circ\text{C}$ during the Etendeka magmatic episode. The youngest ages (~70 Ma) with the longest mean track lengths ($>14 \mu\text{m}$) indicate that a distinct and possibly regional episode of cooling was initiated at around 70 Ma ago. The strong correlation between apatite fission track age and mean confined track length with elevation, indicated by the Okahandja–Swakopmund transect and Gamsberg profile samples (Fig. 5), suggests that the present sample elevations reflect the relative crustal depths of the samples, at least on a local scale, prior to the initiation of cooling. The present erosion surface therefore exposes rocks that were at significantly elevated temperatures at least until ~70 Ma ago which implies that several kilometres of

denudation must have occurred on a regional scale during the Late Mesozoic–Early Tertiary, even allowing for elevated palaeogeothermal gradients of the order of 60°C km^{-1} . This clearly has some important implications for the burial history of the post-glacial Permian erosion surface and the subsequent geomorphic history of northern Namibia.

5. Quantifying the thermal history interpretation

In order to place more quantitative constraints on the proposed post-Damara thermal history a simple 1D numerical thermal model that accounts for magmatic heating and erosion simultaneously (Brown et al., 1994b) was used to explore a range of viable thermal history interpretations. The aim of the thermal modelling was to quantify and explicitly link the thermal history interpretation to a physical process or combination of processes, such as magmatic under plating and intrusion, crustal extension and

thinning and erosion. This strategy is different to the more conventional data driven inversion approach whereby constraints on viable thermal histories are chosen by automatically comparing the goodness of fit between predicted AFTA parameters and the observations alone, without any reference to, or constraint from, the physical processes involved (e.g. Gallagher, 2012). Our aim was to derive the simplest physically based thermal history that was consistent with the quantitative and the qualitative characteristics of the AFTA results, while remaining compatible with other relevant geological and geophysical data. Rather than attempting to reproduce the AFTA results for each sample separately the modelling approach adopted attempted to derive a burial/thermal model that could best reproduce all the observed AFTA results over a discreet crustal section (vertical profile) or region. Our approach follows the rationale outlined by Prenzel et al. (2013) whereby both the geological as well as the thermochronological observations and constraints are used to interpret the AFTA data in terms of the style, chronology and timing of cooling of the crust.

It is unreasonable to expect a simple one dimensional thermal model to be able to satisfy all of the quantitative characteristics of what is essentially a three dimensional data set. In particular, the regional nature of the AFTA data implies they must represent, at least to some extent, lateral variations in the thermal history of the region. However, the thermal effects of regional denudation and magmatic underplating (e.g. Furlong and Fountain, 1986), the two important processes that are incorporated in the thermal models, are themselves regional in nature. If the thermal history of the shallow crust in any particular region is largely controlled by the interaction of these two regional thermal processes then an appropriate one dimensional thermal model should be capable of producing an adequate approximation of the near surface ($<\sim 5$ km) temperature distribution within the crust.

Five different thermal models were derived which were intended to represent the likely thermal histories for five separate but possibly overlapping regions. The models represent a coastal region (area west of the escarpment) an inland region and the northern (Kamanjab region) and southern (Gamsberg profile) margins of the Damara metamorphic belt. The fifth model represents samples that may have been affected by near-surface heating associated with the Etendeka magmatic episode.

5.1. Geological constraints on the post-Damara thermal history

Quantifying the burial history of the present land surface is hindered by the limited amount of information regarding the likely thickness of the denuded Karoo and Etendeka cover sequences. The maximum preserved thickness of ~ 600 m of Karoo age sediments occurs within the Etjo inlier while the thickest preserved section of Etendeka volcanics reaches ~ 800 m at Tafelberg (Marsh et al., 2001). Isolated outcrops of Etendeka(?) lavas occur at elevations of ~ 2000 m, within what appears to be caldera structures, within the Brandberg and Erongo alkaline ring complexes, and the isolated sandstone outcrops, believed to be of Karoo age, which form the summits of Gamsberg and Klein Gamsberg occur at elevations in excess of ~ 2000 m. These outcrops may represent the remnants of a much thicker, and more extensive cover sequence. On the other hand the sub-volcanic intrusives may have been intruded into localised volcanic piles and the Gamsberg block may have been structurally displaced, in which case there is no need to infer a substantially thicker cover sequence. However, the thickness of the Upper Cretaceous sedimentary sequence preserved offshore (Rust and Summerfield, 1990; Rouby et al., 2009; Guillocheau et al., 2012) and the Late Mesozoic palaeotemperatures indicated by the AFTA data mitigate in favour of a more extensive cover sequence, reaching thicknesses of at least several kilometres in places.

In addition to the problems concerning the limited stratigraphic information there is also the problem of choosing, or preferably estimating, an appropriate Late Mesozoic palaeogeothermal gradient. Thermobarometry data from the Damaran metamorphic rocks (Martin and Eder, 1983; Miller, 1983) indicate peak metamorphic palaeogeothermal gradients of $60\text{--}70\ ^\circ\text{C km}^{-1}$ for the central region, and $\sim 20\ ^\circ\text{C km}^{-1}$ for the southern marginal zone (Gamsberg region) of the Damara metamorphic belt. Measurements of radioactive heat production within the Damara granites, which occur largely within the central zone of the belt, are also anomalously high ($4\text{--}8 \times 10^{-6}\text{ W m}^{-3}$) (Haack, 1983). These data prompted Haack (1983) to propose that the Damara granites provided a long-lived radioactive heat source which sustained the lateral variation in peak metamorphic palaeogeothermal gradient through to the present. He suggested that it was this lateral variation in palaeogeothermal gradient that gave rise to the apparent gradient in apatite fission track age across the Okahandja lineament. However, present day heat flow measurements (Ballard et al., 1987) from northern Namibia document a relatively constant geothermal gradient of $18\text{--}24\ ^\circ\text{C km}^{-1}$ across much of the region, despite the anomalous heat production values for the Damaran granites, which mitigates against the proposal for a long-lived lateral variation in geothermal gradient. The maximum palaeotemperatures estimated from the AFTA data (Fig. 5) also suggest that relatively 'normal' thermal gradients ($20\text{--}35\ ^\circ\text{C km}^{-1}$) existed prior to the initiation of Late Mesozoic denudation.

On the other hand, there is some evidence that substantial amounts of basaltic magma were added to the base, or intruded into, the lower crust during the early stages of continental rifting (e.g. White and McKenzie, 1989; Bauer et al., 2000; Fernandez et al., 2010). The addition of large volumes of basaltic magma to the crust would produce a transient increase in the geothermal gradient. The Etendeka volcanic sequence contains a large proportion (~75%) of rhyolitic lavas interbedded with the basaltic lavas (Erlank et al., 1984; Marsh et al., 2001). The geochemistry of the rhyolitic lavas suggests that they were derived from partial melting of Damaran crustal rocks, where as the source of basaltic lavas has been interpreted as being heterogeneously enriched continental lithosphere (Erlank et al., 1984). The source of heat required to produce the observed volume of rhyolitic lavas may well have been the large volumes of basaltic magma (represented by the combined Paraná and Etendeka provinces) generated by lithospheric thinning occurring over the Tristan da Cunha mantle plume, and which were underplated onto or intruded into the lower crust.

Some evidence for basaltic underplating is provided by regional seismic refraction profiles within the Damara mobile belt (Bauer et al., 1983; Bauer et al., 2000). There does not appear to be a well defined crust–mantle seismic transition (Moho) but rather a diffuse boundary occurring over $\sim 10\text{--}15$ km. The velocity profile shows this zone, between approximately 30 km and 45 km depth, to have maximum P wave velocities of between 7.0 and 8.0 km s^{-1} . This type of crustal P wave velocity structure has been interpreted in several other regions as being indicative of magmatic thickening of the crust by underplating of basaltic magmas onto and intrusion into the lower crust (White et al., 1987a,b; White and McKenzie, 1989; Durrheim and Mooney, 1991, 1994; Nguuri et al., 2001).

Additional evidence which supports the basaltic underplating hypothesis comes from petrogenetic arguments which suggest that the Karoo lavas (Central Karoo and Etendeka provinces) evolved to their present compositions by some form of low pressure fractional crystallization process (Marsh and Eales, 1984; Erlank et al., 1984). Following White and McKenzie's (1989) suggestion, that permanent regional surface uplift of northwestern Namibia could have been generated by basaltic underplating following rifting over the Tristan da Cunha mantle plume, Cox (1989) proposed that the present day drainage patterns within northern Namibia form

a roughly radial pattern which he suggested might be reflecting the regional domal uplift caused by the magmatic underplating. However, Gilchrist and Summerfield (1990) argue that drainage patterns are consequent upon the current topography, which reflects many influences that post-date the proposed domal uplift. Analysis of the offshore sedimentary record for the Namibian and South African sectors of the margin also suggest a more complex topographic evolution including post-rift phase/s of uplift and/or major climate change (e.g. Guillocheau et al., 2012).

5.2. The thermal modelling results

The schematic burial histories, for the pre-Karoo unconformity surface, shown in Fig. 9 were based on the limited stratigraphic evidence described above and incorporate two burial phases and one or more denudational phases. The initial burial phase, beginning at 300 Ma, represents the deposition of the Karoo sequence, and the second represents the Etendeka lava sequence beginning at 130 Ma, with maximum burial depths being achieved by 120 Ma. An initial geothermal gradient of $25^{\circ}\text{C km}^{-1}$ was assumed. The thermal effects of the Etendeka magmatism were approximated by simulating the addition of ~ 10 km of basaltic magma to the base of the crust (35 km), between 130 Ma and 120 Ma. It was also assumed that all samples had zero initial age at 500 Ma, but for most samples, the predicted AFTA parameters are relatively insensitive to this initial age. The AFTA results predicted by these models are most sensitive to the maximum palaeotemperatures achieved and the time of cooling from these temperatures. The thermal models were all calculated using the simple one dimensional numerical scheme that was described in detail in Brown et al. (1994b) and were designed with the following important observations in mind:

1. Some areas of the present land surface represent a Late Palaeozoic glacial surface overlain in places by Permo-Carboniferous sediments.
2. Outcropping basement rocks have been exposed to a range of Late Mesozoic palaeotemperatures, which must have exceeded $110^{\circ} \pm 10^{\circ}\text{C}$ for some samples, which imply that substantial denudation must have occurred during the Cretaceous. This is true even if palaeogeothermal gradients were significantly elevated relative to the present values of $18\text{--}24^{\circ}\text{C km}^{-1}$.
3. The AFTA data for many of the samples indicate that accelerated cooling from these palaeotemperatures was initiated at ~ 70 Ma.
4. Limited information from the offshore Walvis basin indicates a thick (>4 km) Late Cretaceous clastic sedimentary section.
5. The limited terrestrial Cenozoic geology indicates a Palaeogene (or older) age for the Namib Unconformity Surface and a significant increase in the rate of denudation of the escarpment region during the Miocene is suggested by the Karpenkliff Conglomerate Formation.

5.2.1. Details of the regional thermal models

The maximum depth of burial in the coastal region model (Fig. 9a) is 2.5 km, and comprises 1.5 km of 'Karoo' sediments and 1 km of 'Etendeka' lavas. Three denudational phases were included. The first between 120 Ma and 75 Ma, immediately following the Etendeka magmatic episode, removing 1 km of section at a rate of $\sim 22\text{ m Ma}^{-1}$. The second denudational phase, between 75 Ma and 65 Ma, removed 2.5 km of section at a rate of 250 m Ma^{-1} , and the last phase from 65 Ma to the present removed 1 km. This implies that 2 km of the total of 4.5 km of denuded section comprised pre-Karoo basement rocks. It seems reasonable to expect that denudation of the coastal region began during the early

stages of continental rifting during the Early Cretaceous, but the AFTA data indicates that most of the cooling occurred at ~ 70 Ma.

The inland region model (Fig. 9a) uses the same burial history as the coastal region model, having a total burial depth of 2.5 km. The total depth of section removed by the two denudational phases is 3 km. The first phase occurs between 75 Ma and 65 Ma and removes 1.5 km of section at a rate of 150 m Ma^{-1} and the second, which begins at 25 Ma, also removes 1.5 km but at a slower rate of 60 m Ma^{-1} . This second phase of denudation is required in order to allow the samples now at the surface to have remained at moderately elevated temperatures after initially cooling at ~ 70 Ma, but it is not well constrained by the AFTA data, and cosmogenic isotope studies (Cockburn et al., 2000; Bierman and Caffee, 2001) indicate that Tertiary erosion rates were likely lower (c. $5\text{--}15\text{ m Ma}^{-1}$) across this region of the margin. The timing of this second denudational phase coincides with the proposed Miocene increase in the rate of denudation of the escarpment region inland of the Kuisib drainage basin (Ward, 1987) and so it is possible there were short lived phases of increased river incision and erosion through the Tertiary, but at a scale undetectable by the AFTA thermochronometer. The Gamsberg region model (Fig. 9b) is identical to the inland region model except that magmatic underplating was not included in the calculation of the thermal history. Magmatic underplating was not included in the Gamsberg model because it is the region most distant from the hypothesised Early Cretaceous location of the Tristan mantle plume, and would thus have been on the periphery of the predicted region of magmatic underplating (White and McKenzie, 1989).

The Kamanjab region model (Fig. 9b) incorporates two burial phases, similar to the other models, but with less section being deposited during each burial phase. The first burial phase represents 1 km of 'Karoo' sediment and the second represents 0.5 km of 'Etendeka' lavas. There is only a single denudational phase which begins at 75 Ma, and removes the 1.5 km section deposited earlier, between then and the present. Magmatic underplating was included for this model. To simulate the thermal history of samples from the central region that may have experienced the more localised effects of the sub-volcanic intrusions, the inland region model was run with the depth of magmatic underplating reduced to only 10 km. While this is clearly an unrealistic underplating scenario, it does provide a means of generating a relatively short lived 'thermal event' similar to that which might be experienced by a sample within the contact aureole of a large magmatic intrusion.

5.2.2. Discussion of the modelling results

The thermal models illustrated in Fig. 9 were used to calculate the thermal histories for a series of successively deeper points, spaced at 250 m intervals, with the first point being at the surface prior to the initiation of the first denudational phase. These series of thermal histories were then used to calculate the AFTA parameters for hypothetical crustal profiles using an apatite fission track annealing model (Laslett et al., 1987). The modelled apparent apatite fission track ages for these profiles are shown in Fig. 10, plotted against initial sample depth, rather than final elevation. This allows an estimated depth of denudation to be read directly from these profile diagrams for any given apparent fission track age. For each sample location, point estimates of the amount of denudation can then be read from the appropriate profile. This procedure is illustrated schematically (Fig. 11) for a generalised north-south and an east-west cross-section. The modelled profiles have been superimposed onto the topographic cross sections such that an appropriate apatite fission track age occurs at the present land surface. Note that the age scale for the 1-dimensional modelled profiles is not equivalent to distance.

We chose to use the Laslett et al. (1987) fission track annealing model and a constant 'standard' apatite composition (Durango

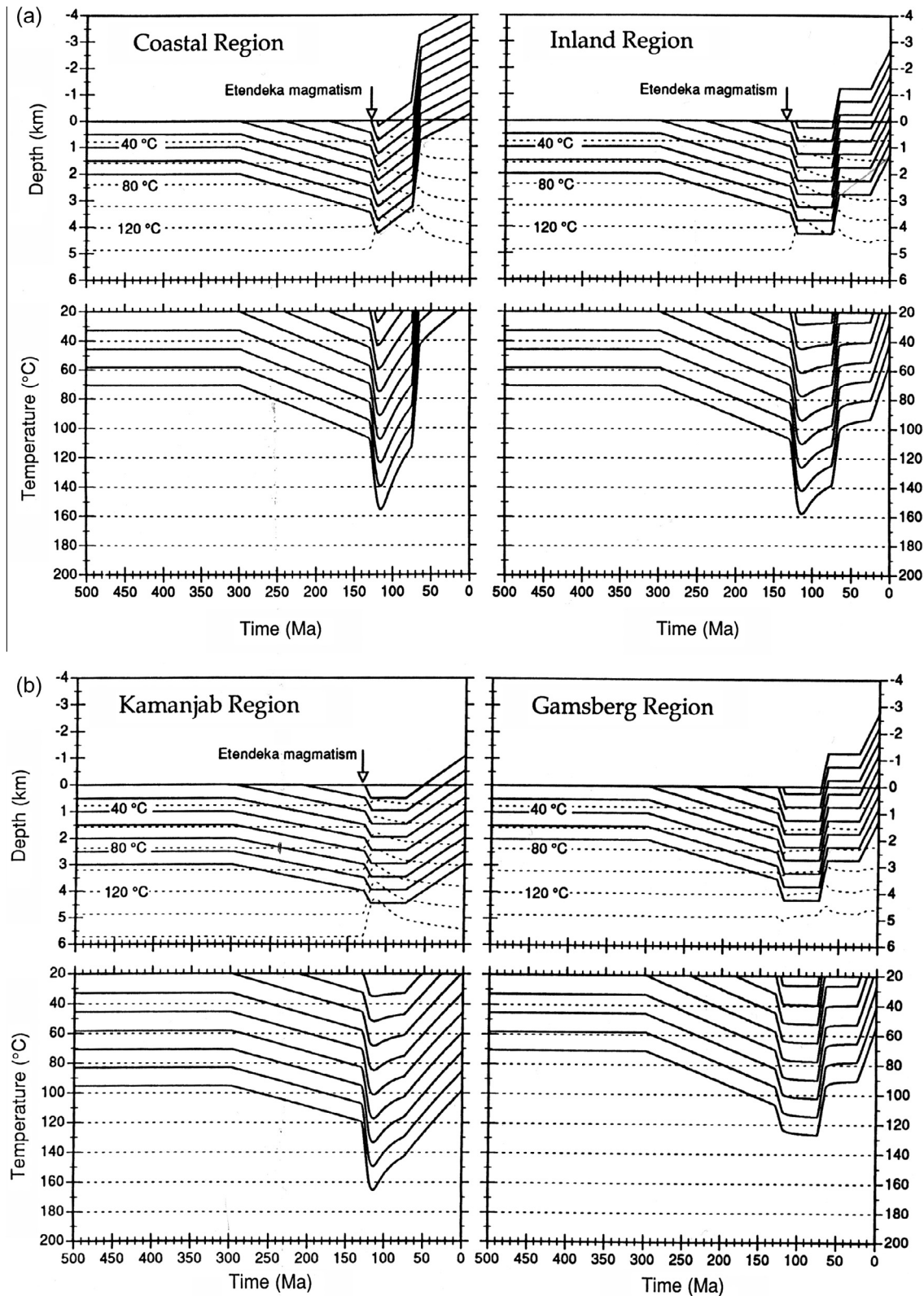


Fig. 9. Burial and thermal histories for the Coastal and Inland (a) models and the Kamanjab and Gamsberg (b) thermal models. Seeing that the maximum depth, and not the detailed burial history, is the most important factor in determining the thermal history in these models the effect of sediment compaction was ignored. Depths to selected isotherms (spaced at 20 °C intervals) are shown on the burial history plots. For all models, except the Gamsberg model, the thermal effects of magmatic underplating (Etendeka magmatism?) cause a transient increase in the thermal gradient and so the isotherms move to shallower depths and subsequently 'relax' back towards their original depth. Note that the advective effect of sedimentation or denudation causes a minor decrease or increase, respectively, in the near surface thermal gradient. The model curves shown represent a vertical series samples regularly spaced at a depth interval of 0.5 km.

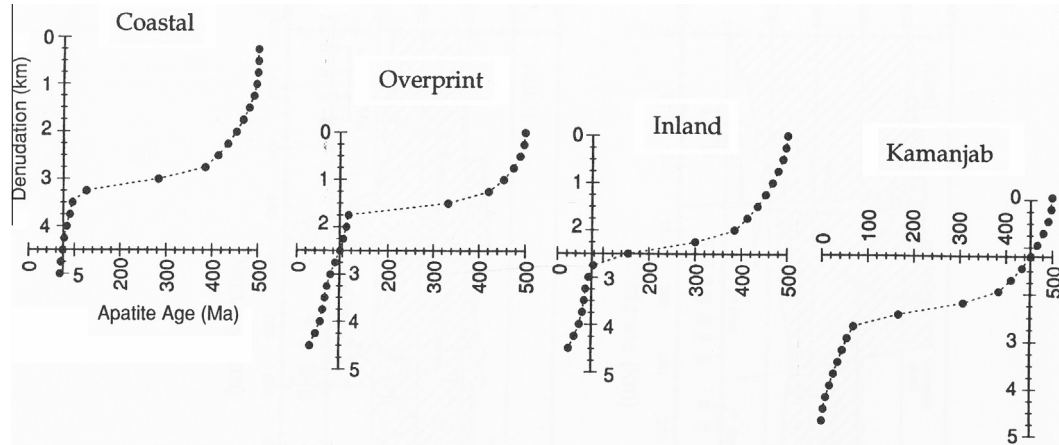


Fig. 10. Modelled apatite fission track age profiles derived from the five thermal models discussed in the text. The profiles are plotted such that the age scale represents the present mean land surface in each region and the vertical scale represents depth below an initial mean land surface appropriate for that region. Measured apatite fission track ages can then be used to derive point estimates of the depth of denudation by reading off the depth of denudation from the appropriate model profile.

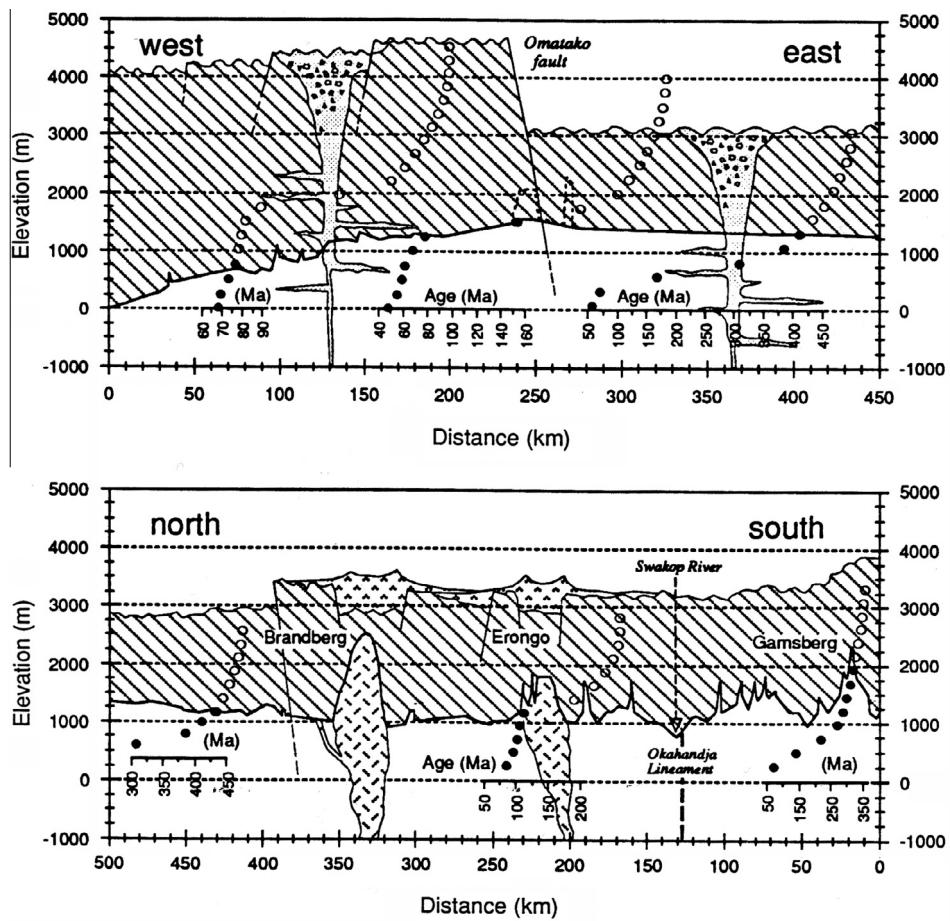


Fig. 11. Schematic topographic and geological cross sections illustrating the relationship between the fission track profiles, the initial land surface and the present land surface. The hatched region represents the estimated depth of Late Mesozoic denudation. Note that the age scale for the modelled apatite fission track age profiles is not equivalent to distance, but indicates the variation of age with depth for a 1-dimensional (vertical) profile.

apatite) for all models and believe this is justified and sensible in this case because it enables the predictions of the different process based thermal histories to be compared between different models, and also between different areas. We do acknowledge though that specific samples may have behaved differently in detail from our 'standard' Durango apatite composition (depending on the actual Cl content of the apatite). However, the purpose of this study

was not to model the thermal histories of each sample site in precise detail, but rather to use the whole data set to try and constrain the broad pattern, and timing, of cooling across the study area in a self consistent manner. From our understanding of the published multi-composition annealing models (e.g. Ketcham et al., 1999, 2007), and our own experience of using these, we believe that the model thermal histories derived here are unlikely to be in error

by more than a maximum of 10 °C or so (likely less), and so any refinement arising from using more complex composition based annealing models will not materially change our key conclusions. We note also that using the form of the age profile, and the time of the so called ‘break-in-slope’ alone, may not be good indicator of the timing of cooling (e.g. Prenzel et al., 2013) and so viable thermal models were constrained using both the form of the profile as well as the goodness of fit of the actual AFTA parameters (i.e. age and track length distributions) for individual samples. Clearly, thermal histories could be derived for the observed data using the more conventional data driven inversion and optimisation approach (e.g. Gallagher, 2012), and this will certainly be the focus of our ongoing work aimed at analysing the more precise detail, subtle variations and spatial patterns of individual sample thermal histories.

For the purpose of comparing the modelled AFTA results with the measured AFTA data from along the Okahandja–Swakopmund transect, a composite model profile was constructed comprising segments from the Coastal, Inland and Kamanjab regional models (Fig. 12). The upper 2 km of the composite profile is taken from the Kamanjab regional model, the middle 2 km from the inland regional model and the lower 2 km section from the coastal model. The two modelled profiles shown for the Gamsberg profile were generated by running the Gamsberg model with an initial age of 500 Ma and 350 Ma, respectively.

Seeing that the Okahandja–Swakopmund transect samples were collected over a horizontal distance of several hundred kilometres (see Fig. 3), and that the point estimates of the depth of denudation for each sample ranges from 4.5 km at the coast to 1.25 km inland, the present sample elevations for these samples do *not* reflect their relative initial depths. To reconstruct the relative initial crustal depths for the Okahandja–Swakopmund transect samples it is necessary to backstack the denuded section (Brown, 1991). This is achieved by calculating the amount of isostatic rebound expected at each sample point, given the estimated denudation at that point, and subtracting this from the present elevation. Having done this, the relative crustal depths can then be normalised in such away as to superimpose the reconstructed profile onto the modelled profile (Fig. 12e and f). When this backstacking procedure is followed a good correspondence is achieved between the composite modelled profile and the measured AFTA data from the Okahandja–Swakopmund transect. The backstacking calculations were conducted using an Airy local isostatic compensation model. The generally good correlation between the modelled AFTA results and the measured AFTA data for this transect provides support for the three proposed thermal history styles incorporated in the composite modelled profile. Further support is provided by the generally good correlation between the predicted and measured distributions of confined track lengths (see Fig. 6a and b).

The samples from the Gamsberg profile were collected over a much smaller horizontal distance (~ 100 km) and the range of point estimates for the depth of denudation for these samples is also relatively small (~ 2.5 to ~ 3.5 km). The amount of isostatic rebound will thus be similar for all these samples and the present sample elevations are therefore likely to closely approximate the relative crustal depths for this profile. For this reason the sample elevations were simply normalised in such a way as to superimpose the measured AFTA data onto the modelled profiles shown in Fig. 12c and d. The elevations for the three highest samples were reduced by 700 m prior to converting the elevations to depths. This assumes that a fault exists between the upper three samples and the lower part of the profile (see Fig. 5). Again, the correspondence

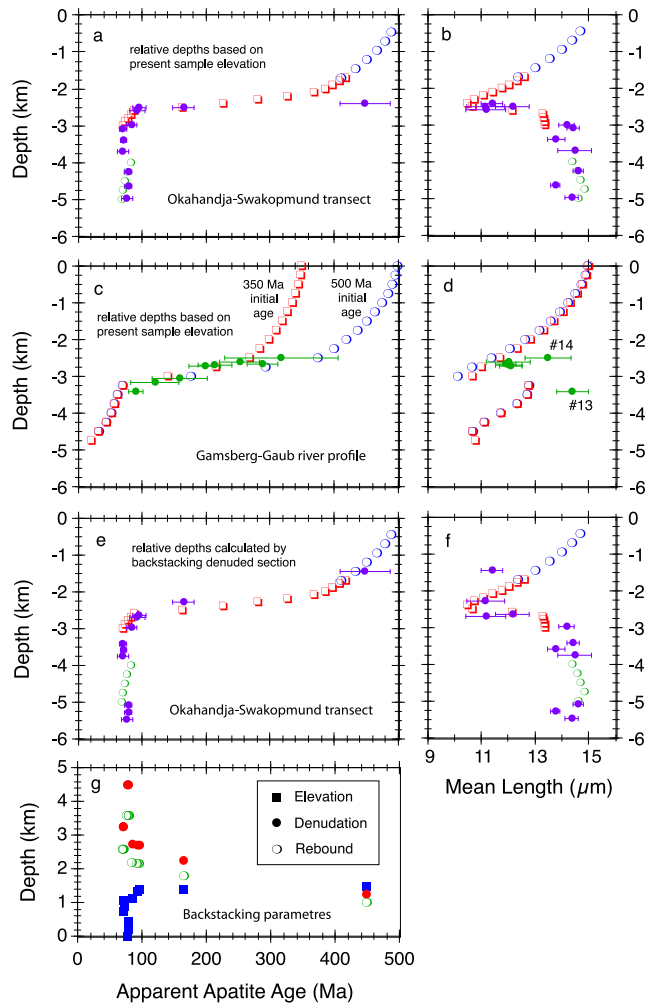


Fig. 12. Comparison between the measured AFTA data (solid symbols) and the model results (open symbols). The modelled AFTA parameters for each of a vertical series of hypothetical samples have been plotted against the maximum depth attained by each sample, that is, the depth prior to the initiation of denudation. The relative ‘depths’ for the measured AFTA data points shown in panels a through d represent the present sample elevations. The sample elevations were normalised so as to superimpose the measured AFTA profiles with the modelled profiles (simply by adding an appropriate constant). The Okahandja–Swakopmund model profile (panels a, b and e, f) is a composite model profile, derived from the Coastal, Inland and Kamanjab models. The upper 2 km section is from the Kamanjab model (large open circles), the middle 2 km section from the Inland model (open squares) and the bottom 2 km section is from the Coastal model (small open circles). The two modelled profiles compared with the Gamsberg–Gaub river profile (c, d) were both derived from the burial history shown in Fig. 9b, but represent initial ages of 350 Ma (open squares) and 500 Ma (open circles), respectively. Note that the lower section (ages $<\sim 300$ Ma) is effectively the same for both of these profiles, indicating that the measured AFTA parameters (for samples analysed) are insensitive to the initial age. The Okahandja–Swakopmund transect was collected over a horizontal distance of ~ 300 km (Fig. 3) and the estimated depth of denudation ranges from ~ 1 km in the interior to $\geq \sim 4\text{--}5$ km at the coast. Consequently, the present, relative sample elevations are unlikely to represent the original relative sample depths because of differential, denudational isostatic rebound of the surface along the transect. The relative depths for the Okahandja–Swakopmund transect samples were adjusted by backstacking the denuded section (predicted by the composite modelled profile in panel a), assuming local isostatic compensation (Brown, 1991). This adjustment simply subtracts the isostatic rebound component from the present sample elevation. The effect of the backstacking adjustment is to ‘stretch out’ the relative sample depths so that depths of younger samples are increased relative to depths of older samples, and thus reinstating the true relative structural depths. Using the backstacked depths for the Okahandja–Swakopmund transect provides a better fit with the modelled profile (panels e and f) than that obtained using the uncorrected depths (panels a and b).

between the modelled AFTA results and the measured data is generally good. However, two of the measured mean confined track lengths are significantly longer than that predicted for the equivalent sample depths. For both these samples the number of track lengths measured is too low (13 and 14 tracks, respectively) to provide an accurate estimate of the mean length. Also, the biased nature of the confined track length measurement procedure (Laslett et al., 1982, 1984; Green, 1988) would be expected to over predict the mean track length for samples with an insufficient number of confined track lengths.

6. Conclusions and geodynamic implications

The fission track data presented in this paper place some important new constraints on the post-Damara thermal history of the shallow crust in northern Namibia. The apatite fission track ages for Damaran metasediments and granites range from ~450 Ma to ~70 Ma, and the relationship between apatite age and the distribution of confined track lengths within each sample, indicates that most of the samples experienced a significant acceleration in cooling rate, beginning at ~70 Ma. The results of the thermal modelling have shown that this episode of cooling must be associated with a substantial increase in the rate of crustal denudation, even if magmatic underplating of the crust, associated with the Etendeka magmatism, had given rise to transient elevated palaeogeothermal gradients.

The total depth of Late Mesozoic denudation, implied by the range of maximum palaeotemperatures estimated from the AFTA results, varies from over 4.5 km near the coast to about ~1 km for inland regions. These estimates of the depth of denudation require a much more extensive and thicker Karoo sedimentary and/or Etendeka lava sequence than is presently preserved in northern Namibia, given that the present land surface represents

a pre-Karoo glacial surface in places. This has important implications for original extent of the Paraná-Etendeka flood basalt province, implying as it does that the present asymmetry in the distribution of the volcanic rocks between southeastern Brazil and Namibia may be more apparent than real. This apparent asymmetry, generated by differential denudation, between the volumes of basalt represented by the Etendeka and Paraná volcanic provinces was also referred to by Cox (1989).

The timing of accelerated cooling (and denudation) post-dates the initial rifting leading to the opening of the South Atlantic oceanic basin by about 50 Ma, and is broadly synchronous with the Late Cretaceous episode of transcontinental, intraplate deformation documented in West, Central and East Africa. The cause of this deformation has been attributed to the stresses, resulting from differential opening between the Central and South Atlantic ocean basins, being transferred along oceanic fracture zones and dissipated as a combination of strike slip and extensional faulting within the continental interior (e.g. Fairhead, 1988; Fairhead and Binks, 1991; Binks and Fairhead, 1992). The coincidence between this period of plate motion change, within the South Atlantic Ocean basin, and the accelerated crustal cooling documented within northern Namibia, suggests a causative link between these two episodes. The distinctive spatial pattern (Fig. 13) and timing of cooling recorded within the Damara region of Namibia indicates that intracontinental deformation similar to that documented elsewhere in Africa at this time extended into the southern sub-Saharan African continent. This deformation may well enable resolution of the geometric problems related to misfit/overlap between South America and Africa for plate tectonic models of the South Atlantic (e.g. Eagles, 2007; Torsvik et al., 2009; Aslanian et al., 2009; Aslanian and Moulin, 2012).

If the dominant period of cooling at ~70 Ma occurred in response to an acceleration in denudation rate at this time, it follows that a significant increase in the mean topographic relief

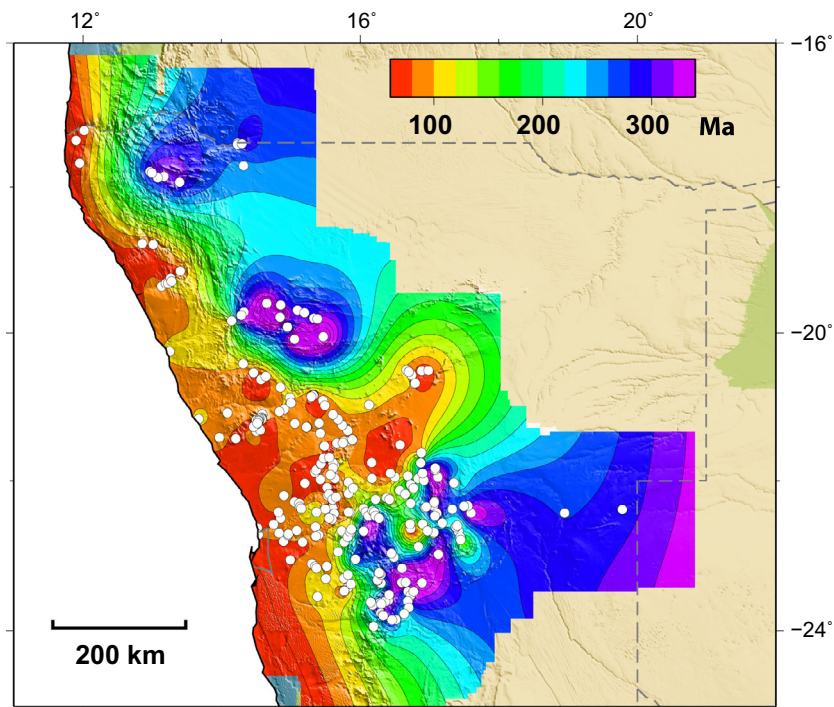


Fig. 13. Map illustrating the pattern of apatite fission track age across northern Namibia. The map was generated for the combined results from this study and published data from Haack (1976, 1983), Luft et al. (2005), Raab (2001) and Raab et al. (2002, 2005). On a regional scale there is a remarkable correlation between the pattern of apatite fission track age and the regional NE-SW structural trend of the Damara metamorphic belt. The youngest ages occur along the coast and within the central region of the Damara metamorphic belt further inland and the ages increase towards the north and the south. The age pattern shown here, and the discrete timing of cooling during the Late Cretaceous, synchronous with similar intracontinental deformation elsewhere in Africa, suggest that reactivation of the regional structures have influenced the denudation pattern and hence low temperature thermal history of the crust in northern Namibia.

must have also occurred at this time, given that local relief appears to be the dominant control on denudation rate (Ahnert, 1970; Pinet and Souriau, 1988; Summerfield, 1991). Increased local relief, caused by tectonic reactivation of these pre-existing basement structures, could therefore be invoked as a viable cause of the proposed acceleration in the rate of denudation. A similar argument was used to explain the substantial (5–6 km) Pleistocene denudation of the King Range, which occurs along the San Andreas transform fault in southern California, implied by the very young (<1 Ma) apatite fission track ages from this region (Dumitru et al., 1991).

As proposed by Moore et al. (2008) and Jelsma et al. (2009) reactivation of these lithospheric scale structures, during the Late Cretaceous, also provides an explanation for the patterns of occurrence of kimberlitic and other related alkaline magmatism within southern Africa at this time (Marsh, 1973; Moore, 1976), such as the Gibeon kimberlite field in central Namibia (Reid et al., 1990). Small to moderate amounts of lithospheric extension and thinning and hence decompression, associated with the intracontinental deformation, may be sufficient to produce the low degrees of partial melting required for the generation of alkaline (kimberlitic) magmas. Particularly, seeing that the mantle beneath central Namibia may have been anomalously hot due to the presence of the Vema and Discovery mantle plumes beneath this region at ~70 Ma (Reid et al., 1990). Also, the reactivation of the steep, lithospheric scale structures would provide access for the eruption of these magmas, although this is not necessarily required by some small fraction melt segregation models (McKenzie, 1985). This broad correlation between timing of phases of kimberlite emplacement in southern Africa and accelerated phases of erosion during the early and late-mid Cretaceous has been documented elsewhere in South Africa (Tinker et al., 2008).

The broad correlation between the regional distribution of apatite fission track ages and major tectonic structures in northern Namibia (Fig. 13) supports the view that reactivation of these structures had an important influence on the Late Mesozoic thermal history of the crust. Our new data, combined with previous results and the thermal modelling constraints provide a robust and important first order measure of the scale and style of Late Cretaceous tectonism within southern Africa, and suggest that other segments of the Damara–Okavango–Mwembeshi shear zones may have also been reactivated during this period.

Acknowledgements

The samples analyses during this study were collected during several field programs and the authors acknowledge the considerable logistic and financial support received from the Namibian Geological Survey and also from De Beers Consolidated Mines Ltd. Mike Deihl, John Ward, Mike de Wit and Simon Milner are all thanked for their generous and significant input, field expertise and assistance at various times. Insightful discussions with Matthias Raab, and his assistance with assembling the regional data set is also gratefully acknowledged. This work was supported by research Grant NE/H008276/1 from the Natural Environment Research Council, United Kingdom.

Appendix A. Supplementary material

Supplementary data associated with this article can be found, in the online version, at <http://dx.doi.org/10.1016/j.jafrearsci.2014.05.014>.

References

- Ahnert, F., 1970. Functional relationships between denudation, relief and uplift in large mid-latitude drainage basins. *Am. J. Sci.* 268, 243–263.
- Almeida, F.F.M.de, Hasui, Y., De Brito Neves, B.B., 1976. The Upper Precambrian of South America. *Inst. Geosci. Univ. São Paulo Bolet.* 7, 45–80.
- Aslanian, D., Moulin, M., 2012. Palaeogeographic consequences of conservative models in the South Atlantic Ocean. *Geol. Soc. London* 369. <http://dx.doi.org/10.1144/SP369.5>, Special Publications.
- Aslanian, D., Moulin, M., Olivet, J.L., Unternehr, P., Matias, L., Bache, F., Labails, C., 2009. Brazilian and African passive margins of the Central Segment of the South Atlantic Ocean: kinematic constraints. *Tectonophysics* 468 (1), 98–112.
- Austin Jr, J.A., Uchupi, E., 1982. Continental-oceanic crustal transition off Southwest Africa. *AAPG Bull.* 66 (9), 1328–1347.
- Baier, B., Berckhemer, H., Gajewski, D., Green, R.W., Grimsel, C., Prodehl, C., Vees, R., 1983. Deep seismic sounding in the area of the Damara Orogen, Namibia, south west Africa. In: *Intracontinental Fold Belts*. Springer, Berlin Heidelberg, pp. 885–900.
- Ballard, S., Pollack, H.N., Skinner, N.J., 1987. Terrestrial heat flow in Botswana and Namibia. *J. Geophys. Res.* 92, 6291–6300.
- Barnes, S.J., Sawyer, E.W., 1980. An alternative model for the Damara Mobile Belt: ocean crust subduction and continental convergence. *Precambr. Res.* 13, 297–336.
- Barton Jr, J.M., Key, R.M., 1981. The tectonic development of the Limpopo mobile belt and the evolution of the Archean cratons of Southern Africa. In: Kröner, A. (Ed.), *Precambrian Plate Tectonics*. Elsevier, Amsterdam, pp. 185–212.
- Basu, T.N., Shrivastava, B.B.P., 1981. Structure and Tectonics of Gondwana Basins in Peninsular India: Gondwana Five. Balkema, Rotterdam, pp. 177–182.
- Bauer, K., Neben, S., Schreckenberger, B., Emmermann, R., Hinz, K., Fechner, N., Weber, K., 2000. Deep structure of the Namibia continental margin as derived from integrated geophysical studies. *J. Geophys. Res.* 105 (B11), 25829–25853.
- Bierman, P.R., Caffee, M., 2001. Slow rates of rock surface erosion and sediment production across the Namib Desert and escarpment, southern Africa. *Am. J. Sci.* 301 (4–5), 326–358.
- Binks, R.M., Fairhead, J.D., 1992. A plate tectonic setting for Mesozoic rifts of West and Central Africa. *Tectonophysics* 213, 141–151.
- Blundell, D.J., 1976. Active faults in West Africa. *Earth Planet. Sci. Lett.* 31, 287–290.
- Bois, C., Lefort, J.P., Le Gall, B., Sibuet, J.C., Gariel, O., Pinet, B., Cazes, M., 1990. Superimposed Variscan, Caledonian and Proterozoic features inferred from deep seismic profiles recorded between southern Ireland, southwestern Britain and western France. *Tectonophysics* 177, 15–37.
- Bosworth, W., 1992. Mesozoic and early Tertiary rift tectonics in East Africa. *Tectonophysics* 209 (1), 115–137.
- Brown, R.W., 1991. Backstacking apatite fission track 'stratigraphy': a method for resolving the erosional and isostatic rebound components of tectonic uplift histories. *Geology* 19, 74–77.
- Brown, R.W., Summerfield, M.A., Gleadow, A.J., 1994a. Apatite fission track analysis: Its potential for the estimation of denudation rates and implications for models of long-term landscape development. *Proc. Models Theor. Geomorphol.*, 24–53.
- Brown, R., Gallagher, K., Duane, M., 1994b. A quantitative assessment of the effects of magmatism on the thermal history of the Karoo sedimentary sequence. *J. Afr. Earth Sci.* 18 (3), 227–243.
- Bufford, K.M., Atekwana, E.A., Abdelsalam, M.G., Shemang, E., Atekwana, E.A., Mickus, K., Molwalefhe, L., 2012. Geometry and faults tectonic activity of the Okavango Rift Zone, Botswana: Evidence from magnetotelluric and electrical resistivity tomography imaging. *J. Afr. Earth Sci.* 65, 61–71.
- Burke, K.C., 1976a. Development of graben associated with the initial ruptures of the Atlantic Ocean. *Tectonophysics* 36, 93–111.
- Burke, K.C., 1976b. The Chad Basin: an active intra-continental basin. *Tectonophysics* 36, 197–206.
- Burke, K.C., Dewey, J.F., 1974. Two plates in Africa during the Cretaceous? *Nature* 249, 313–316.
- Cande, S.C., La Brecque, J.L., Haxby, W.F., 1988. Plate kinematics of the South Atlantic: chron 34 to present. *J. Geophys. Res.* 93, 13479–13492.
- Castaing, C., 1991. Post-Pan-African tectonic evolution of South Malawi in relation to the Karroo and Recent East African Rift Systems. *Tectonophysics* 191, 55–73.
- Clemson, J., Cartwright, J., Booth, J., 1997. Structural segmentation and the influence of basement structure on the Namibian passive margin. *Journal of the Geological Society* 154 (3), 477–482.
- Cockburn, H.A.P., Brown, R.W., Summerfield, M.A., Seidl, M.A., 2000. Quantifying passive margin denudation and landscape development using a combined fission-track thermochronology and cosmogenic isotope analysis approach. *Earth Planet. Sci. Lett.* 179 (3), 429–435.
- Cordani, U.G., Amaral, G., Kawashita, K., 1973. The Precambrian evolution of South America. *Geol. Rundsch.* 62, 309–317.
- Coward, M.P., Daly, M.C., 1984. Crustal lineaments and shear zones in Africa: their relationship to plate movements. *Precambr. Res.* 24, 27–45.
- Cox, K.G., 1989. The role of mantle plumes in the development of continental drainage patterns. *Nature* 342, 873–877.
- Cox, K.G., Johnson, R.L., Monkman, L.J., Stillman, C.J., Vail, J.R., Wood, D.N., Wood, D.N., 1965. The geology of the Nuanetsi igneous province. *Philos. Trans. R. Soc. London Ser. A, Math. Phys. Sci.* 257 (1078), 71–218.
- Dallmeyer, R.D., 1990. 40Ar/39Ar mineral age record of the polyorogenic evolution within the Seve and Koli nappes, Trondelag. *Tectonophysics* 179, 199–226.
- Dallmeyer, R.D., Lecorche, J.P., 1990. 40Ar/39Ar polyorogenic mineral age record in the northern Mauritanide orogen, West Africa. *Tectonophysics* 177, 81–107.
- Daly, M.C., Chorowicz, J., Fairhead, J.D., 1989. Rift basin evolution in Africa: the influence of reactivated steep basement shear zones. In: Cooper, M.A., Williams, G.D. (Eds.), *Inversion Tectonics*. Geological Society Special Publication No. 44, pp. 309–334.

- Daly, M.C., Lawrence, S.R., Kimun'a, D., Binga, M., 1991. Late Palaeozoic deformation in central Africa: a result of distant collision? *Nature* 350, 605–607.
- De Swardt, A.M.J., Garrard, P., Simpson, J.G., 1965. Major zones of transcurrent dislocation and superposition of orogenic belts in part of central Africa. *Bull. Geol. Soc. Am.* 76, 89–102.
- de Vera, J., Granado, P., McClay, K., 2010. Structural evolution of the Orange Basin gravity-driven system, offshore Namibia. *Mar. Pet. Geol.* 27 (1), 223–237.
- Dingle, R.V., Siesser, W.G., Newton, A.R., 1983. Mesozoic and Tertiary Geology of Southern Africa. A.A. Balkema, Rotterdam, 375 pp.
- Downing, K.N., Coward, M.P., 1981. The Okahandja Lineament and its significance for Damaran tectonics in Namibia. *Geol. Rundsch.* 70, 972–1000.
- Dumitru, T.A., Hill, K.C., Coyle, D.A., Duddy, I.R., Foster, D.A., Gleadow, A.J.W., Green, P.F., Kohn, B.P., Laslett, G.M., O'Sullivan, A.J., 1991. Fission track thermochronology: Application to continental rifting of south-eastern Australia. *Aust. Petrol. Exploration Association J.* 31, 131–142.
- Durrheim, R.J., Mooney, W.D., 1991. Archean and Proterozoic crustal evolution: evidence from crustal seismology. *Geology* 19 (6), 606–609.
- Durrheim, R.J., Mooney, W.D., 1994. Evolution of the Precambrian lithosphere: seismological and geochemical constraints. *J. Geophys. Res.* 99 (B8), 15359–15374.
- Dypvik, H., Nesteby, H., Ruden, F., Aagaard, P., Johansson, T., Msundai, J., Massay, C., 1990. Upper Paleozoic and Mesozoic sedimentation in the Rukwa-Tukuyu region, Tanzania. *J. Afr. Earth Sci.* 11, 437–456.
- Eales, G., 2007. New angles on South Atlantic opening. *Geophys. J. Int.* 168 (1), 353–361.
- Eales, H.V., Marsh, J.S., Cox, K.G., 1984. The Karoo igneous province: an introduction. In: Erlank, A.J. (Ed.), Petrogenesis of the Volcanic Rocks of the Karoo Province. Special Publication of the Geological Society of South Africa, No. 13, pp. 1–26.
- Erlank, A.J., 1984. Petrogenesis of the volcanic rocks of the Karoo province. Special Publication of the Geological Society of South Africa, No. 13, 395 pp.
- Erlank, A.J., Marsh, J.S., Duncan, A.R., Miller, R. McG., Hawkesworth, C.J., Betton, P.J., Rex, D.C., 1984. Geochemistry and petrogenesis of the Etendeka volcanic rocks from SWA/Namibia. In: Erlank, A.J. (Ed.), Petrogenesis of the Volcanic Rocks of the Karoo Province. Special Publication of the Geological Society of South Africa, No. 13, pp. 195–246.
- Fairhead, J.D., 1988. Mesozoic plate reconstructions of the Central-South Atlantic Ocean: the role of the West and Central African Rift System. *Tectonophysics* 155, 181–191.
- Fairhead, J.D., Binks, R.M., 1991. Differential opening of the Central and South Atlantic Oceans and the opening of the West African rift system. *Tectonophysics* 187, 191–203.
- Fairhead, J.D., Henderson, N.B., 1977. The seismicity of southern Africa and incipient rifting. *Tectonophysics* 41, 19–26.
- Fairhead, J.D., Okereke, C.S., 1987. A regional gravity study of the West African Rift System in Nigeria and Cameroon and its tectonic interpretation. *Tectonophysics* 143, 141–159.
- Fernandez, M., Afonso, J.C., Ranalli, G., 2010. The deep lithospheric structure of the Namibian volcanic margin. *Tectonophysics* 481 (1), 68–81.
- Fielding, C.R., Webb, J.A., 1996. Facies and cyclicity of the Late Permian Bainmedart Coal Measures in the Northern Prince Charles Mountains, MacRobertson Land, Antarctica. *Sedimentology* 43 (2), 295–322.
- Fishwick, S., Bastow, I.D., 2011. Towards a better understanding of African topography: a review of passive-source seismic studies of the African crust and upper mantle. *Geol. Soc. London* 357 (1), 343–371, Special Publications.
- Fitch, F.J., Miller, J.A., 1984. Dating Karoo igneous rocks by the conventional K-Ar and 40Ar/39Ar age spectrum methods. In: Erlank, A.J. (Ed.), Petrogenesis of the Volcanic Rocks of the Karoo Province. Special Publication of the Geological Society of South Africa, No. 13, pp. 247–266.
- Foster, D.A., Gleadow, A.J., 1992. The morphotectonic evolution of rift-margin mountains in central Kenya: constraints from apatite fission-track thermochronology. *Earth Planet. Sci. Lett.* 113 (1), 157–171.
- Foster, D.A., Gleadow, A.J., 1993. Episodic denudation in East Africa: a legacy of intracontinental tectonism. *Geophys. Res. Lett.* 20 (21), 2395–2398.
- Foster, D.A., Gleadow, A.J., 1996. Structural framework and denudation history of the flanks of the Kenya and Anza Rifts. *East Africa. Tectonics* 15 (2), 258–271.
- Francheteau, J., Le Pichon, X., 1972. Marginal fracture zones as structural framework of continental margins in the South Atlantic Ocean. *Am. Assoc. Pet. Geol. Bull.* 56, 991–1007.
- Fuller, A.O., 1971. South Atlantic fracture zones and lines of old weakness in Southern Africa. *Nature* 231, 84–85.
- Fuller, A.O., 1972. Possible fracture zones and rifts in southern Africa. *Geol. Soc. Am. Mem.* 132, 159–172.
- Furlong, K.P., Fountain, D.M., 1986. Continental crustal underplating: thermal considerations and seismic-petrologic consequences. *J. Geophys. Res.* 91 (B8), 8285–8294.
- Galbraith, R.F., 1988. Graphical display of estimates having differing standard errors. *Tecometrics* 30, 271–281.
- Galbraith, R.F., 1990. The radial plot: graphical assessment of spread in ages. *Nucl. Tracks Radiat. Meas.* 17, 207–214.
- Gallagher, K., 2012. Transdimensional inverse thermal history modeling for quantitative thermochronology. *J. Geophys. Res.: Solid Earth* 117 (B2). <http://dx.doi.org/10.1029/2011JB008825> (1978–2012).
- Gallagher, K., Brown, R., Johnson, C., 1998. Fission track analysis and its applications to geological problems. *Annu. Rev. Earth Planet. Sci.* 26 (1), 519–572.
- Gevers, T.W., 1936. The Etjo Beds of northern Hereroland, South West Africa. *Trans. Geol. Soc. South Africa* 48, 27–29 (in Dingle 1983).
- Gilchrist, A.R., Summerfield, M.A., 1990. Differential denudation and flexural isostasy in formation of rifted-margin upwarps. *Nature* 346, 739–742.
- Gleadow, A.J.W., 1981. Fission-track dating methods: what are the real alternatives? *Nuclear Tracks* 5 (1), 3–14.
- Gleadow, A.J., Brown, R.W., 2000. Fission-track thermochronology and the long-term denudational response to tectonics. *Geomorphol. Global Tectonics*, 57–75.
- Gray, D.R., Foster, D.A., Goscombe, B., Passchier, C.W., Trouw, R.A., 2006. 40Ar/39Ar thermochronology of the Pan-African Damara Orogen, Namibia, with implications for tectonothermal and geodynamic evolution. *Precambr. Res.* 150 (1), 49–72.
- Green, P.F., 1985. Comparison of zeta calibration baselines for fission track dating of apatite, zircon and sphene. *Chem. Geol. (Isotope Geosci. Section)* 58, 1–22.
- Green, P.F., 1988. The relationship between track shortening and fission track age reduction in apatite: Combined influences of inherent instability, annealing anisotropy, length bias and system calibration. *Earth Planet. Sci. Lett.* 89, 335–352.
- Green, D., Crockett, R.N., Jones, M.T., 1980. Tectonic control of Karoo sedimentation in mid-eastern Botswana. *Trans. Geol. Soc. South Africa* 83, 213–219.
- Guillocheau, F., Rouby, D., Robin, C., Helm, C., Rolland, N., Le Carlier de Veslud, C., Braun, J., 2012. Quantification and causes of the terrigenous sediment budget at the scale of a continental margin: a new method applied to the Namibia-South Africa margin. *Basin Res.* 24 (1), 3–30.
- Guiraud, R., Maurin, J.C., 1992. Early Cretaceous rifts of Western and Central Africa: an overview. *Tectonophysics* 213 (1), 153–168.
- Guiraud, R., Binks, R.M., Fairhead, J.D., Wilson, M., 1992. Chronology and geodynamic setting of Cretaceous-Cenozoic rifting in West and Central Africa. *Tectonophysics* 213 (1), 227–234.
- Haack, U., 1976. Rekonstruktion der Abkühlungsgeschichte des Damara-Orogen in Südwest-Afrika mit Hilfe von Spaltspuren-Altern. *Geol. Rundsch.* 65 (1), 967–1002.
- Haack, U., 1983. Reconstruction of the cooling history of the Damara Orogen by correlation of radiometric ages with geography and altitude. In: Martin, H., Eder, F.W. (Eds.), *Intracontinental Fold Belts*. Springer-Verlag, Berlin, pp. 873–884.
- Hammerbeck, E.C.I., Allcock, I.J., 1985. 1:4000000 Geological Map of Southern Africa. Geological Society of South Africa.
- Hartnady, C.J.H., 1974. An ERTS-1 view of the south western part of the Damara Mobile Belt. *Precambrian Research Unit of the University of Cape Town Annual Report*, vol. 12, p. 60.
- Hartnady, C.J.H., 1979. Overthrust tectonics, stratigraphic problems and metallogenesis in the Khomas Ridge Province, Damara orogenic belt. *Precambrian Research Unit of the University of Cape Town Annual report*, vol. 16, p. 73–89.
- Henry, G., Clendenin, C.W., Stanistreet, I.G., Maiden, K.J., 1990. Multiple detachment model for the early rifting stage of the Late Proterozoic Damara orogen in Namibia. *Geology* 18 (1), 67–71.
- Holzflörster, F., Stollhofen, H., Stanistreet, I.G., 1999. Lithostratigraphy and depositional environments in the Waterberg-Erongo area, central Namibia, and correlation with the main Karoo Basin, South Africa. *J. Afr. Earth Sci.* 29 (1), 105–123.
- Hunter, D.R., 1981. *Precambrian of the Southern Hemisphere*. Elsevier.
- Hurford, A.J., Green, P.F., 1983. The zeta age calibration of fission-track dating. *Chem. Geol. (Isotope Geosci. Section)* 1, 285–317.
- Jelsma, H., Barnett, W., Richards, S., Lister, G., 2009. Tectonic setting of kimberlites. *Lithos* 112, 155–165.
- Jerram, D.A., Mountney, N., Stollhofen, H., 1999. Facies architecture of the Etjo Sandstone Formation and its interaction with the Basal Etendeka Flood Basalts of northwest Namibia: implications for offshore prospectivity. *Geol. Soc. London* 153 (1), 367–380, Special Publications.
- Jerram, D.A., Mountney, N.P., Howell, J.A., Long, D., Stollhofen, H., 2000. Death of a sand sea: an active aeolian erg systematically buried by the Etendeka flood basalts of NW Namibia. *J. Geol. Soc.* 157 (3), 513–516.
- Kampunzu, A.B., Kapenda, D., Manteka, B., 1991. Basic magmatism and geotectonic evolution of the Pan African belt in central Africa: evidence from the Katangan and West Congolian segments. *Tectonophysics* 190, 363–371.
- Keith Martin, A., Hartnady, C.J., Goodlad, S.W., 1981. A revised fit of South America and south central Africa. *Earth Planet. Sci. Lett.* 54 (2), 293–305.
- Kennedy, W.Q., 1964. The Structural Differentiation of Africa in the Pan African (± 500 m.y.) Tectonic Episode. University of Leeds, Research Institute of African Geology, Department of Earth Sciences Annual Report, vol. 8, p. 48–49.
- Ketcham, R.A., Donelick, R.A., Carlson, W.D., 1999. Variability of apatite fission-track annealing kinetics: III. Extrapolation to geological time scales. *Am. Mineral.* 84, 1235–1255.
- Ketcham, R.A., Carter, A., Donelick, R.A., Barbarand, J., Hurford, A.J., 2007. Improved modeling of fission-track annealing in apatite. *Am. Mineral.* 92 (5–6), 799–810.
- Kinabo, B.D., Atekwana, E.A., Hogan, J.P., Modisi, M.P., Wheaton, D.D., Kampunzu, A.B., 2007. Early structural development of the Okavango rift zone, NW Botswana. *J. Afr. Earth Sci.* 48 (2), 125–136.
- Kinabo, B.D., Hogan, J.P., Atekwana, E.A., Abdelsalam, M.G., Modisi, M.P., 2008. Fault growth and propagation during incipient continental rifting: Insights from a combined aeromagnetic and Shuttle Radar Topography Mission digital elevation model investigation of the Okavango Rift Zone, northwest Botswana. *Tectonics* 27 (3), TC3013.
- Kitgord, K.D., Schouten, H., 1986. Plate kinematics of the Central Atlantic. In: Tucholke, B.E., Vogt, P.P. (Eds.), *The Geology of North America*, Vol. M: The Western North Atlantic Region, Geological Society of America, Boulder, Colorado, pp. 351–378.

- Kröner, A., 1977. Precambrian mobile belts of southern and eastern Africa—Ancient sutures or sites of ensialic mobility? A case for crustal evolution towards plate tectonics. *Tectonophysics* 40, 101–135.
- Kröner, A., 1980. Pan African crustal evolution. *Episodes* 2, 3–8.
- Kukla, P.A., Stanistreet, I.G., 1991. Record of the Damaran Khomas Hochland accretionary prism in central Namibia: refutation of an “ensialic” origin of a Late Proterozoic orogenic belt. *Geology* 19, 473–476.
- Laslett, G.M., Kendall, W.S., Gleadow, A.J.W., Duddy, I.R., 1982. Bias in measurement of fission track length distributions. *Nucl. Tracks Rad. Meas.* 6, 79–85.
- Laslett, G.M., Gleadow, A.J.W., Duddy, I.R., 1984. The relationship between fission track length and track density in apatite. *Nucl. Tracks Rad. Meas.* 9, 29–38.
- Laslett, G.M., Green, P.F., Duddy, I.R., Gleadow, A.J.W., 1987. Thermal annealing of fission tracks in apatite, 2. A quantitative analysis. *Chem. Geol. (Isotope Geosci. Section)* 65, 1–13.
- Le Pichon, X., Fox, P.J., 1971. Marginal offsets, fracture zones, and the early opening of the North Atlantic. *J. Geophys. Res.* 76 (26), 6294–6308.
- Loule, J.-P., Pospisil, L., 2012. Geophysical evidence of Cretaceous volcanics in Logone Birni Basin (Northern Cameroon), Central Africa, and consequences for the West and Central African Rift System. *Tectonophysics*. doi:10.1016/j.tecto.2012.10.021.
- Luft, F.F., Luft Jr, J.L., Chemale Jr, F., Lelarge, M.L.M.V., Ávila, J.N., 2005. Post-Gondwana break-up record constraints from apatite fission track thermochronology in NW Namibia. *Radiat. meas.* 39 (6), 675–679.
- Manspeizer, W., 1988. Triassic-Jurassic Rifting: Continental Breakup and the Origin of the Atlantic Ocean and Passive Margins. *Developments in Geotectonics*, vol. 22. Elsevier, New York, 998 pp.
- Marsh, J.S., 1973. Relationships between transform directions and alkaline igneous rock lineaments in Africa and South America. *Earth Planet. Sci. Lett.* 18, 317–323.
- Marsh, J.S., 2010. The geochemistry and evolution of Palaeogene phonolites, central Namibia. *Lithos* 117 (1), 149–160.
- Marsh, J.S., Eales, H.V., 1984. The chemistry and petrogenesis of igneous rocks of the Karoo central area, southern Africa. In: Erlank, A.J. (Ed.), *Petrogenesis of the Volcanic Rocks of the Karoo Province*, Spec. Publ. Geol. Soc. S. Afr, vol. 13, pp. 27–68.
- Marsh, J.S., Ewart, A., Milner, S.C., Duncan, A.R., Miller, R.M., 2001. The Etendeka Igneous Province: magma types and their stratigraphic distribution with implications for the evolution of the Paraná-Etendeka flood basalt province. *Bull. Volcanol.* 62 (6), 464–486.
- Martin, H., 1953. Notes on the Dwyka succession and on some pre-Dwyka valleys in South West Africa. *Trans. Geol. Soc. S. Afr.* 56, 37–43.
- Martin, H., 1976. A geodynamic model for the evolution of the continental margin of southwestern Africa. *Annals of the Brazilian Acad. Sci.* 48, 169–177.
- Martin, A.K., 1984. Propagating rifts: crustal extension during continental rifting. *Tectonics* 3, 611–617.
- Martin, A.K., 1987. Plate reorganisations around Southern Africa, hot-spots and extinctions. *Tectonophysics* 142, 309–316.
- Martin, H., Eder, F.W., 1983. Intracontinental Fold Belts: case studies in the Variscan Belt of Europe and the Damara Belt in Namibia. Springer-Verlag, Berlin.
- Martin, H., Porada, H., 1977a. The intercratonic branch of the Damara orogen South West Africa. Part I. Discussion of geodynamic models. *Precambr. Res.* 5, 311–338.
- Martin, H., Porada, H., 1977b. The intercratonic branch of the Damara orogen South West Africa. Part II. Discussion of relationships with the Pan-African mobile belt system. *Precambr. Res.* 5, 339–357.
- Maurin, J.C., Guiraud, R., 1993. Basement control in the development of the Early Cretaceous West and Central African rift system. *Tectonophysics* 228 (1), 81–95.
- McConnel, R.B., 1980. A resurgent taphrogenic lineament of Precambrian origin in Eastern Africa. *J. Geol. Soc. London* 137, 483–489.
- McHargue, T.R., Heidrick, T.L., Livingston, J.E., 1992. Tectonostratigraphic development of the interior Sudan rifts, Central Africa. *Tectonophysics* 213 (1), 187–202.
- McKenzie, D., 1985. The extraction of magma from the crust and mantle. *Earth Planet. Sci. Lett.* 74 (1), 81–91.
- Miller, R.McG., 1979. The Okahandja Lineament, a fundamental tectonic boundary in the Damara Orogen of South West Africa/Namibia. *Trans. Geol. Soc. South Africa* 82, 349–361.
- Miller, R.McG., 1983. Evolution of the Damara Orogen of South West Africa/Namibia. Geological Society of South Africa Special Publication 11, 515 pp.
- Milner, S., Le Roex, A.P., O'Connor, J.M., 1995. Age of Mesozoic igneous rocks in northwestern Namibia, and their relationship to continental breakup. *J. Geol. Soc.* 152, 97–104.
- Modisi, M.P., 2000. Fault system at the southeastern boundary of the Okavango Rift. Botswana. *J Afr. Earth Sci.* 30 (3), 569–578.
- Modisi, M.P., Atekwana, E.A., Kampunzu, A.B., Ngwisanzi, T.H., 2000. Rift kinematics during the incipient stages of continental extension: Evidence from the nascent Okavango rift basin, northwest Botswana. *Geology* 28 (10), 939–942.
- Moore, A.E., 1976. Controls of post-Gondwana alkaline volcanism in southern Africa. *Earth Planet. Sci. Lett.* 31, 291–296.
- Moore, A., Blenkinsop, T., Cotterill, F.W., 2008. Controls on post-Gondwana alkaline volcanism in Southern Africa. *Earth Planet. Sci. Lett.* 268 (1), 151–164.
- Nguuri, T.K., Gore, J., James, D.E., Webb, S.J., Wright, C., Zengeni, T.G., Snook, J.A., 2001. Crustal structure beneath southern Africa and its implications for the formation and evolution of the Kaapvaal and Zimbabwe cratons. *Geophys. Res. Lett.* 28 (13), 2501–2504.
- Nichols, G.J., Daly, M.C., 1989. Sedimentation in an intracratonic extensional basin: the Karoo of the Central Morondava Basin, Madagascar. *Geol. Mag.* 126, 339–354.
- Nürnberg, D., Müller, R.D., 1991. The tectonic evolution of the South Atlantic from Late Jurassic to Present. *Tectonophysics* 191, 27–53.
- O'Connor, J.M., Duncan, R.A., 1990. Evolution of the Walvis ridge-Rio Grande rise hot spot system: implications for African and South American plate motions over plumes. *J. Geophys. Res.* 95, 17475–17502.
- O'Connor, J.M., le Roex, A.P., 1992. South Atlantic hot spot-plume systems: 1. Distribution of volcanism in time and space. *Earth Planet. Sci. Lett.* 113 (3), 343–364.
- Ollier, C.D., 1977. Outline geological and geomorphological history of the Central Namib Desert. *Modoqua* 10, 207–212.
- Ollier, C.D., 1978. Insebergs of the Namib Desert-processes and history. *Zeitschrift für Geomorphologie Supplementbandt* 31, 161–176.
- Peate, D. W., 1997. The Paraná-Etendeka Province. Large Igneous Provinces: Continental, Oceanic, and Planetary Flood Volcanism, pp. 217–245.
- Peate, D.W., Hawkesworth, C.H., Mantovani, M.S.M., Shukowsky, W., 1990. Mantle plumes and flood-basalt stratigraphy in the Parana, South America. *Geology* 18, 1223–1226.
- Pindell, J.L., Dewey, J.F., 1982. Permo-Triassic reconstructions of western Pangea and the evolution of the Gulf of Mexico/Caribbean region. *Tectonics* 1, 179–211.
- Pinet, P., Souriau, M., 1988. Continental erosion and large-scale relief. *Tectonics* 7, 563–582.
- Porada, H., 1979. The Damara-Ribeira orogen of the Pan-African Brasiliano cycle in Namibia (South-west Africa) and Brazil as interpreted in terms of continental collision. *Tectonophysics* 57, 237–265.
- Porada, H., 1989. Pan-African rifting and orogenesis in southern to equatorial Africa and eastern Brazil. *Precambrian Res.* 44 (2), 103–136.
- Prenzel, J., Lisker, F., Balestrieri, M.L., Läufer, A., Spiegel, C., 2013. The Eisenhower Range, Transantarctic Mountains: evaluation of qualitative interpretation concepts of thermochronological data. *Chem. Geol.* 352, 176–187.
- Priestley, K., McKenzie, D., Debayle, E., Pilidou, S., 2008. The African upper mantle and its relationship to tectonics and surface geology. *Geophys. J. Int.* 175 (3), 1108–1126.
- Raab, M.J., 2001. The Geomorphic Response of the Passive Continental Margin of Northern Namibia to Gondwana Break-Up and Global Scale Tectonics, Doctoral dissertation, Niedersächsische Staats-und Universitätsbibliothek Göttingen, 256pp.
- Raab, M.J., Brown, R.W., Gallagher, K., Carter, A., Weber, K., 2002. Late Cretaceous reactivation of major crustal shear zones in northern Namibia: constraints from apatite fission track analysis. *Tectonophysics* 349 (1), 75–92.
- Raab, M.J., Brown, R.W., Gallagher, K., Weber, K., Gleadow, A.J.W., 2005. Denudational and thermal history of the Early Cretaceous Brandberg and Okenyena igneous complexes on Namibia's Atlantic passive margin. *Tectonics* 24 (3), TC3006. <http://dx.doi.org/10.1029/2004TC001688>.
- Rabinowitz, P.D., La Brecque, J.L., 1979. The Mesozoic South Atlantic Ocean and evolution of its continental margins. *J. Geophys. Res.* 84, 5973–6002.
- Reeves, C.V., 1972. Rifting in the Kalahari? *Nature* 237, 95–96.
- Reeves, C.V., 1978. A failed Gondwana spreading axis in southern Africa. *Nature* 273, 222.
- Reeves, C.V., Hutchins, D.G., 1975. New data on crustal structures in central southern Africa. *Nature* 254, 408–410.
- Reid, D.L., Cooper, A.F., Rex, D.C., Harmer, R.E., 1990. Timing of post-Karoo alkaline volcanism in southern Namibia. *Geol. Mag.* 127, 427–433.
- Reiners, P.W., Brandon, M.T., 2006. Using thermochronology to understand orogenic erosion. *Annu. Rev. Earth Planet. Sci.* 34, 419–466.
- Reiners, P.W., Ehlers, T.A., Zeitler, P.K., 2005. Past, present, and future of thermochronology. *Rev. Mineral. Geochem.* 58 (1), 1–18.
- Ring, U., Kröner, A., Buchwaldt, R., Toukeridis, T., Layer, P.W., 2002. Shear-zone patterns and eclogite-facies metamorphism in the Mozambique belt of northern Malawi, east-central Africa: implications for the assembly of Gondwana. *Precambr. Res.* 116 (1), 19–56.
- Rosenthal, B.R., 1987. Architecture of continental rifts with special reference to East Africa. *Ann. Rev. Earth Planet. Sci.* 15, 445–503.
- Rouby, D., Bonnet, S., Guillocheau, F., Gallagher, K., Robin, C., Bianotto, F., Braun, J., 2009. Sediment supply to the Orange sedimentary system over the last 150 My: an evaluation from sedimentation/denudation balance. *Mar. Pet. Geol.* 26 (6), 782–794.
- Rust, D.J., Summerfield, M.A., 1990. Isopach and borehole data as indicators of rifted margin evolution in southwestern Africa. *Mar. Pet. Geol.* 7, 277–287.
- Sénant, J., Popoff, M., 1991. Early Cretaceous extension in northeast Brazil related to the South Atlantic opening. *Tectonophysics* 198, 35–46.
- Shaw, P.R., Cande, S.C., 1990. High-resolution Inversion for South Atlantic plate kinematics using joint altimeter and magnetic anomaly data. *J. Geophys. Res.* 95, 2625–2644.
- Siesser, W.G., 1978. Aridification of the Namib Desert: evidence from oceanic cores. In: Van Zinderen Bakker, E.M. (Ed.), *Antarctic Glacial History and World Palaeoenvironments*. Balkema, Rotterdam, pp. 105–113.
- Siesser, W.G., 1980. Late Miocene origin of the Benguela upwelling system off northern Namibia. *Science* 208, 283–285.
- Stump, E., 1992. The Ross orogen of the Transantarctic Mountains in light of the Laurentia-Gondwana split. *GSA Today* 2 (2), 25–31.
- Summerfield, M.A., 1991. Sub-aerial denudation of passive margins: regional elevation versus local relief models. *Earth Planet. Sci. Lett.* 102 (3), 460–469.

- Sykes, L.R., 1978. Intraplate seismicity, reactivation of pre-existing zones of weakness, alkaline magmatism and other tectonism post-dating continental fragmentation. *Rev. Geophys. Space Phys.* 16, 621–688.
- Tankard, A.J., Jackson, M.P., Eriksson, K.A., Hobday, D.K., Hunter, D.R., Minter, W.E.L., 1982. Crustal Evolution of Southern Africa: 38 Billion Years of Earth History. Springer-Verlag, New York, 523 pp.
- Tinker, J., de Wit, M., Brown, R., 2008. Linking source and sink: evaluating the balance between onshore erosion and offshore sediment accumulation since Gondwana break-up, South Africa. *Tectonophysics* 455 (1), 94–103.
- Torsvik, T.H., Rousse, S., Labails, C., Smethurst, M.A., 2009. A new scheme for the opening of the South Atlantic Ocean and the dissection of an Aptian salt basin. *Geophys. J. Int.* 177 (3), 1315–1333.
- Trumbull, R.B., Reid, D.L., de Beer, C., van Acken, D., Romer, R.L., 2007. Magmatism and continental breakup at the west margin of southern Africa: a geochemical comparison of dolerite dikes from northwestern Namibia and the Western Cape. *S. Afr. J. Geol.* 110 (2–3), 477–502.
- Unternehr, P., Curie, D., Olivet, J.L., Goslin, J., Beuzart, P., 1988. South Atlantic fits and intraplate boundaries in Africa and South America. *Tectonophysics* 155, 169–179.
- Visser, J.N.J., 1987. The palaeogeography of part of southwestern Gondwana during the Permo-Carboniferous glaciation. *Palaeogeogr. Paleoclim. Palaeoecol.* 61, 205–219.
- Ward, J.D., 1987. The Cenozoic succession in the Kuisib Valley, Central Namib Desert. Geological Survey of South West Africa/Namibia, Memoir 9, 124 pp.
- Ward, J.D., 1988. Geology of the Tsondab Sandstone Formation. *J. Sedim. Geol.* 55, 143–162.
- Ward, J.D., Martin, H., 1987. A terrestrial conglomerate of Cretaceous age—A new record from the Skeleton Coast, Namib Desert. *Commun. Geol. Survey South West Africa/Namibia* 3, 57–58.
- Watters, B.R., 1976. Possible Late Precambrian subduction zone in South West Africa. *Nature* 259, 471–473.
- White, R., McKenzie, D.P., 1989. Magmatism at rift zones: the Generation of volcanic continental margins and flood basalts. *J. Geophys. Res.* 94, 7685–7729.
- White, R.S., Spence, G.D., Fowler, S.R., McKenzie, D.P., Westbrook, G.K., Bowen, A.N., 1987a. Magmatism at rifted continental margins. *Nature* 330, 439–444.
- White, R.S., Westbrook, G.K., Fowler, S.R., Spence, G.D., Barton, P.J., Joppen, M., Morgan, J., Bowen, A.N., Prestcott, C., Bott, M.H.P., 1987b. Hatton Bank (northwest U.K.) continental margin structure. *Geophys. J. Roy. Astron. Soc.* 89, 265–272.
- Winn Jr, R.D., Steinmetz, J.C., Kerekgaryarto, W.L., 1993. Stratigraphy and rifting history of the mesozoic-cenozoic Anza rift, Kenya. *AAPG Bull.* 77 (11), 1989–2005.
- Wopfner, H., 1988. Permo-Triassic sedimentary basins in Australia and East Africa and their relationship to Gondwanic stress pattern. *Gondwana Seven Symposium Volume*, São Paulo, Brazil, p. 133–146.
- Wopfner, H., Kaaya, C.Z., 1991. Stratigraphy and morphotectonics of Karoo deposits of the northern Selous Basin, Tanzania. *Geol. Mag.* 128 (04), 319–334.